Supplementary Materials for Nonparametric Adjustment for Measurement Error in Time to Event Data: Application to Risk Prediction Models

WEB APPENDIX A: ADDITIONAL SIMULATION RESULTS MENDELIAN RISK PREDICTION MODELS

Web Figure 1 compares the three predictions, corresponding to the fifth row in Table 1 (in the main text), representing a simulation setting with sensitivity 0.649 and specificity 0.990. The first column on the left, shows predictions based on error-free family history compared to error-prone family history. The majority of the families have carrier probabilities less than 0.2, therefore we present a close up of these families in the second row. There is more underreporting of cancer (in the plot these are individuals who are below the 45^o line), due to the lower sensitivity. We have many individuals close to the 45^o line, corresponding to simulated families for which error-prone and error-free family histories were very similar. The second column in the middle, shows predictions based on error-free family history compared to our adjustment. In families with high carrier probabilities, we see more individuals below the 45^o line, implying our adjustment method slightly over adjusts by shifting probabilities down. Even though this is the case, overall, model calibration is improved (Table 1 in the main text). We see in the bottom row, for families with lower carrier probabilities, we see individuals both above and below the 45^o. Thus, although it appears that our adjustment method over adjusts for some individuals, the overall O/E shows improvement in calibration. The third column on the right, shows predictions based on error-prone family history compared to our adjustment. We can see that in families with lower carrier probabilities, our adjustment shifts some individuals' carrier probabilities up and some down.

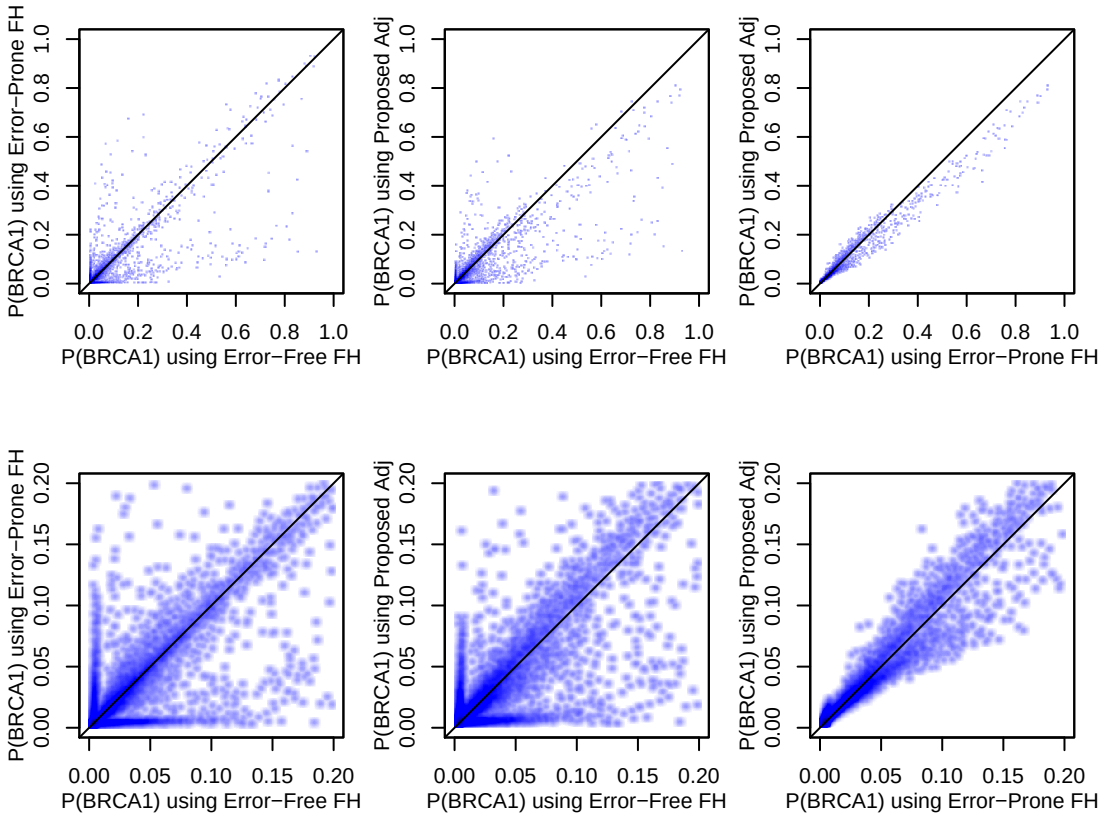

Figure 1: P(BRCA1) for simulated families based on error-free family history, error-prone family history, and the proposed adjustment. In purple, a simulation setting with sensitivity 0.649 and specificity 0.990, classical additive model for error in age $T^* = T + \varepsilon$ where $\varepsilon \sim N(0, 5^2)$, and the counselee is the mother. The bottom row is a close up version of the top row, focusing on counselees with carrier probabilities less than 0.2.

WEB APPENDIX B: ADDITIONAL DESCRIPTION OF MISREPORTING OF AGES IN UCI DATA

Figure 2 shows validated versus reported ages for breast cancer in female relatives in the UCI data. We agree that the simulation setting with a multiplicative measurement error model is not representative of the error-rates in the UCI data (see Figure 2 below) (although could be applicable to other data sources). The additive measurement error model is not completely representative of the error-rates either (as seen below), likely a combination of additive and multiplicative measurement error would be best representative.

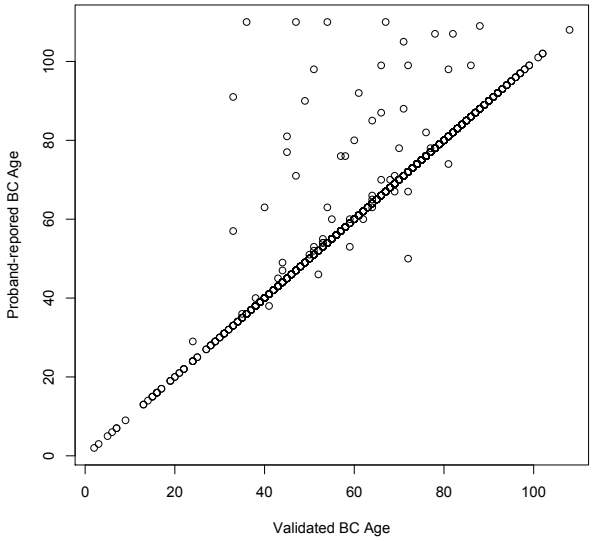

Figure 2: Validated versus Reported Ages for Breast Cancer in Female Relatives in UCI Data.

WEB APPENDIX C: ADDITIONAL SIMULATION RESULTS SURVIVAL PREDICTION MODELS

We conduct additional simulations in the context of the survival prediction models to assess the performance of our proposed adjustment as the sample size of the validation study varies. We

consider a validation study of size $N = 50, 100, 200, 400, 800$ and around 55% censoring. Results, presented in Web Figures 3-14 based on 100 iterations for each sample size, show similar performance of the proposed adjustment when $N = 100, 200, 400, 800$. Boxplots of the proposed adjustment as N varies are shown in Web Figures 15-26, and show that the variability in the estimates decreases slightly as N increases. For the setting when $N = 50$ there were some data generations in which only one out of 50 individuals had $\delta^*_{ttp} = 1$, and therefore it was not possible to estimate $P(T_{ttp}, \delta_{ttp} | T^*_{ttp}, \delta^*_{ttp})$ under these settings.

We conduct additional simulations in the context of the survival prediction models to assess the performance of our proposed adjustment as the bandwidth varies. We consider bandwidths $0.1, \ldots, 0.9$. Results, presented in Web Figures 27-53 based on 100 iterations for each sample size, show similar performance of the proposed adjustment across the bandwidths in terms of MSEP, ROC-AUC, and O/E when bandwidths are less than 0.5. As we increase the bandwidth we still see similar performance of the proposed adjustment in terms of O/E, but MSEP and ROC-AUC become more and more similar to the time independent adjustment, and very similar when the bandwidth is 0.9.

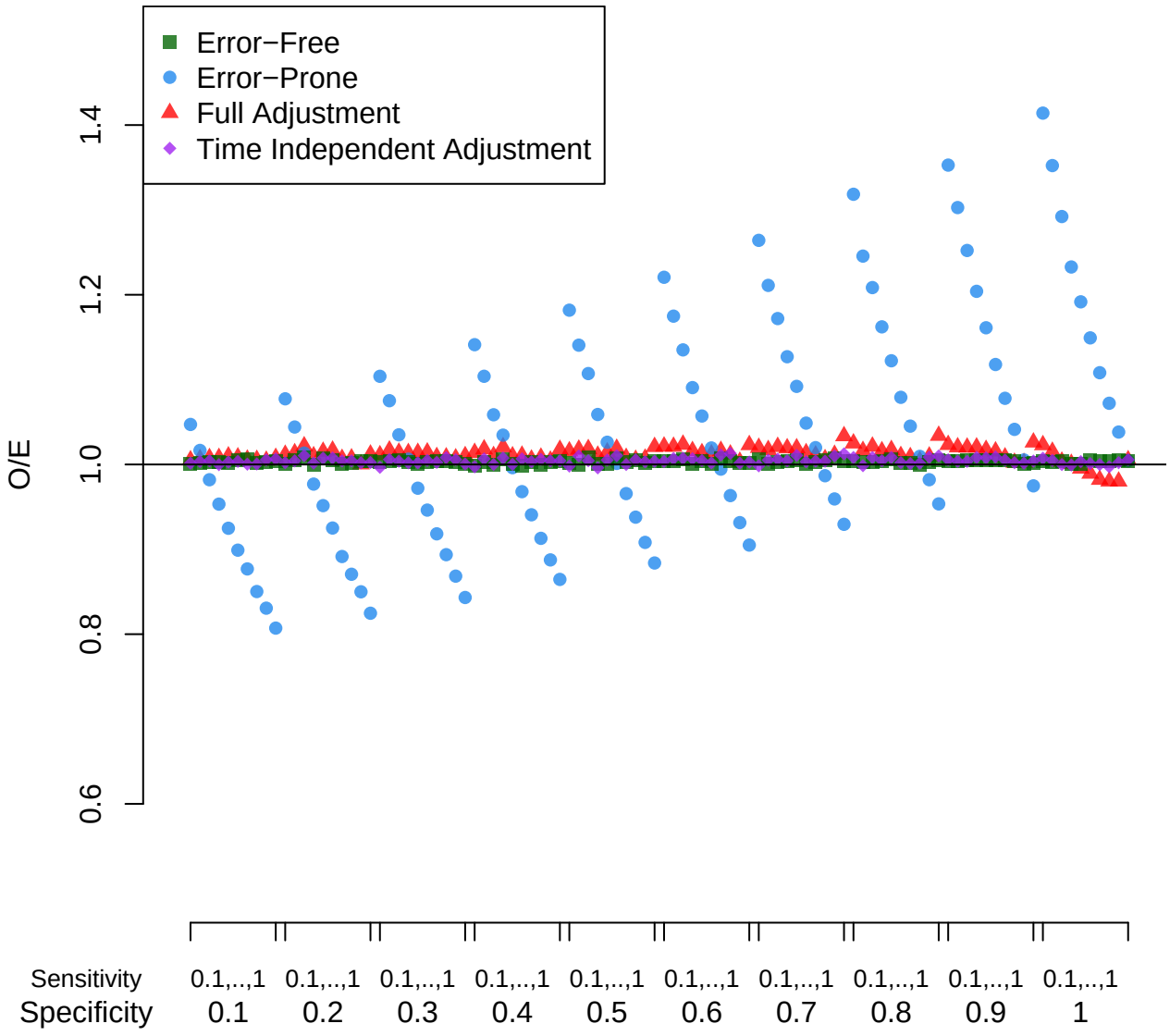

Figure 3: O/E ratios for survival simulations under varying sensitivity and specificity rates, n=100.

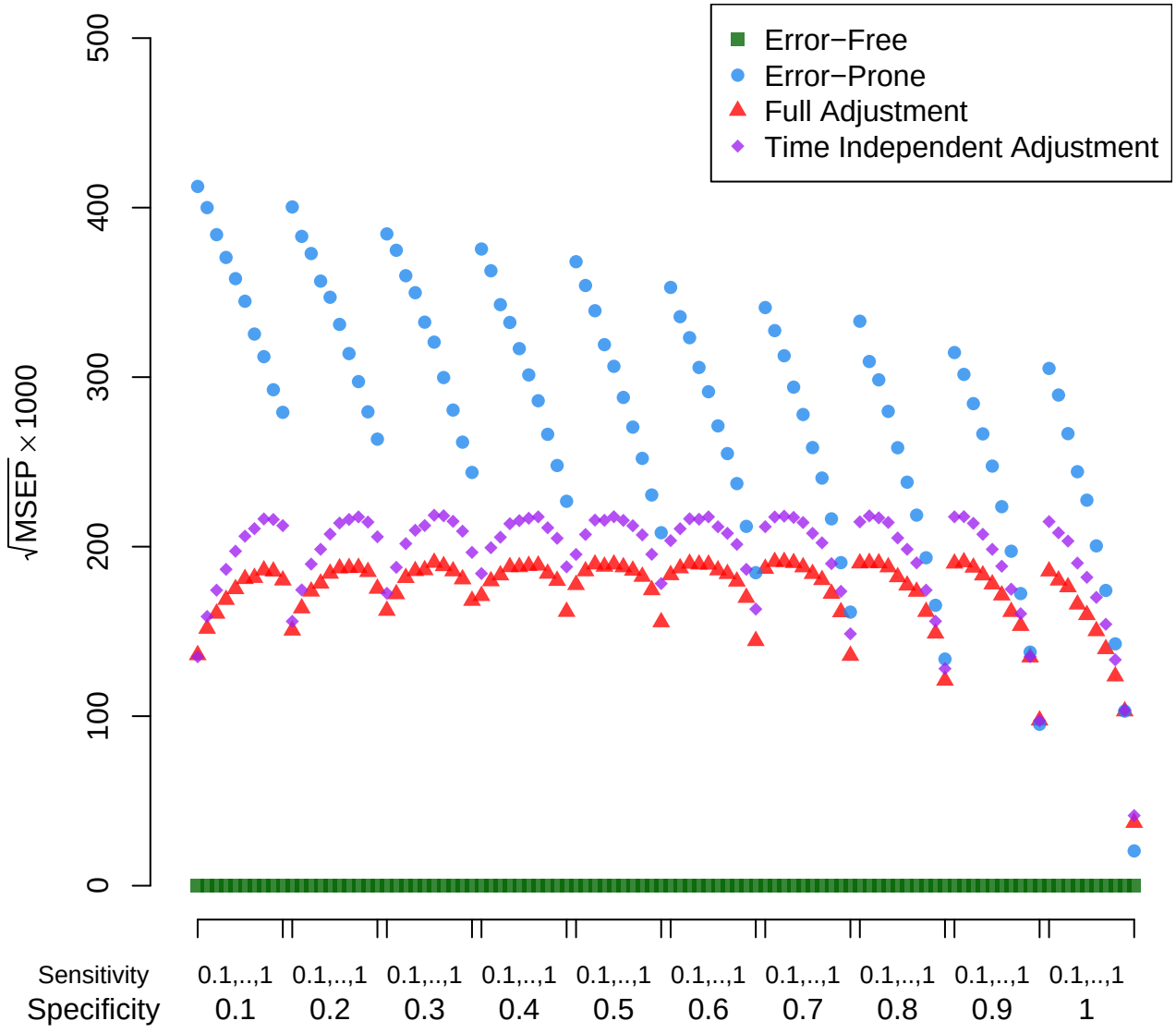

Figure 4: $\sqrt{MSEP} * 1000$ for survival simulations under varying sensitivity and specificity rates, n=100.

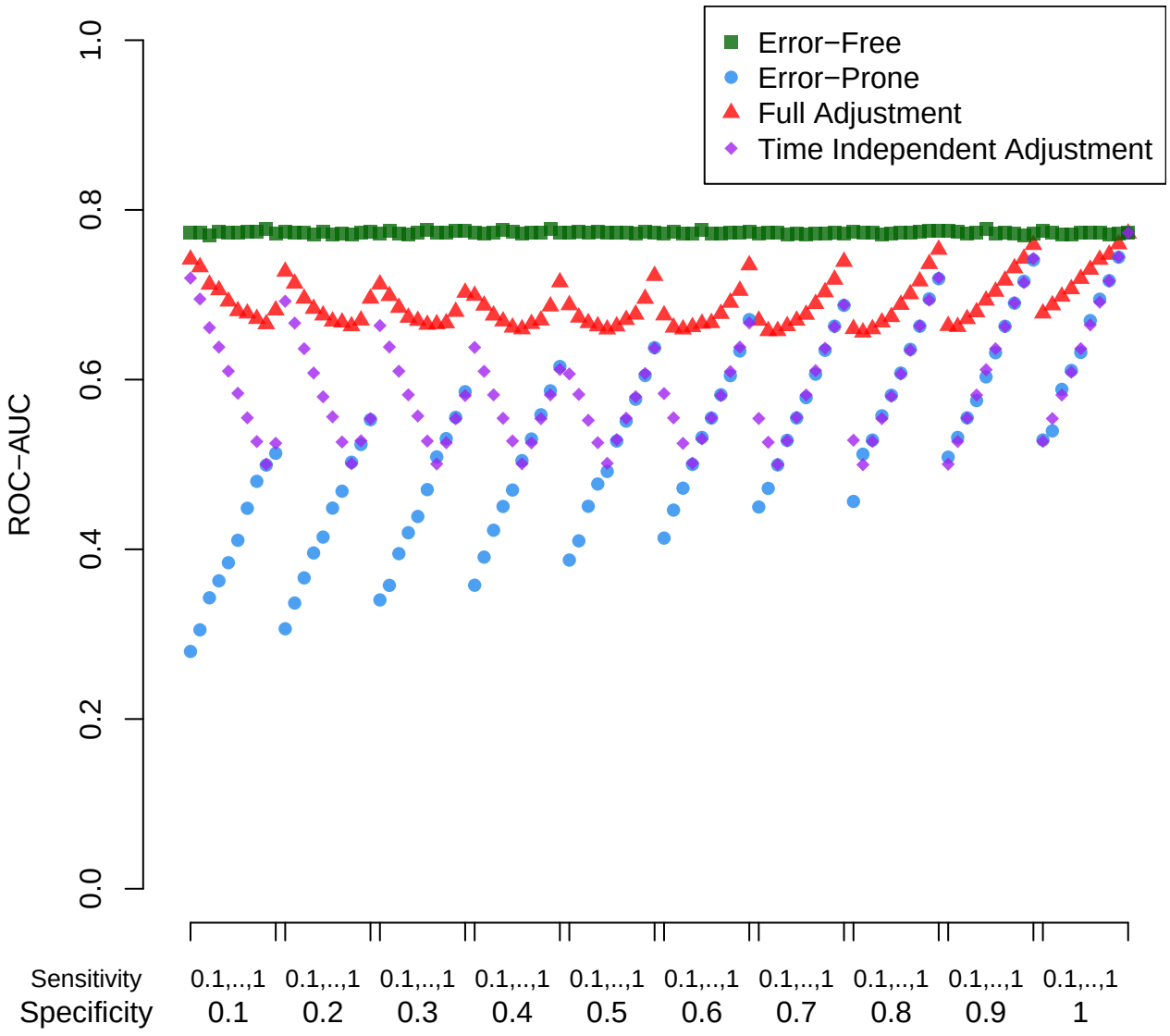

Figure 5: ROC-AUC for survival simulations under varying sensitivity and specificity rates, n=100.

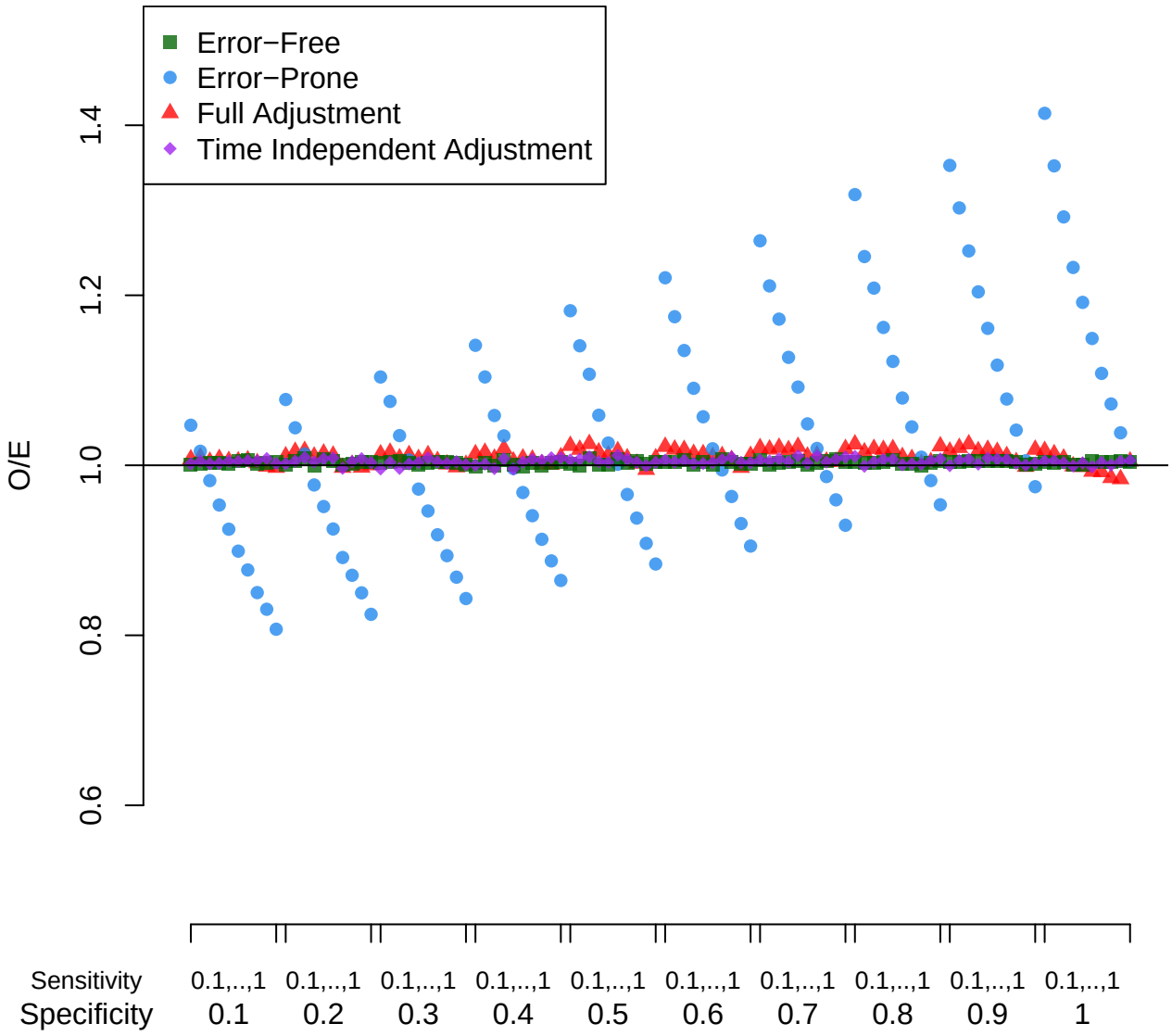

Figure 6: O/E ratios for survival simulations under varying sensitivity and specificity rates, n=200.

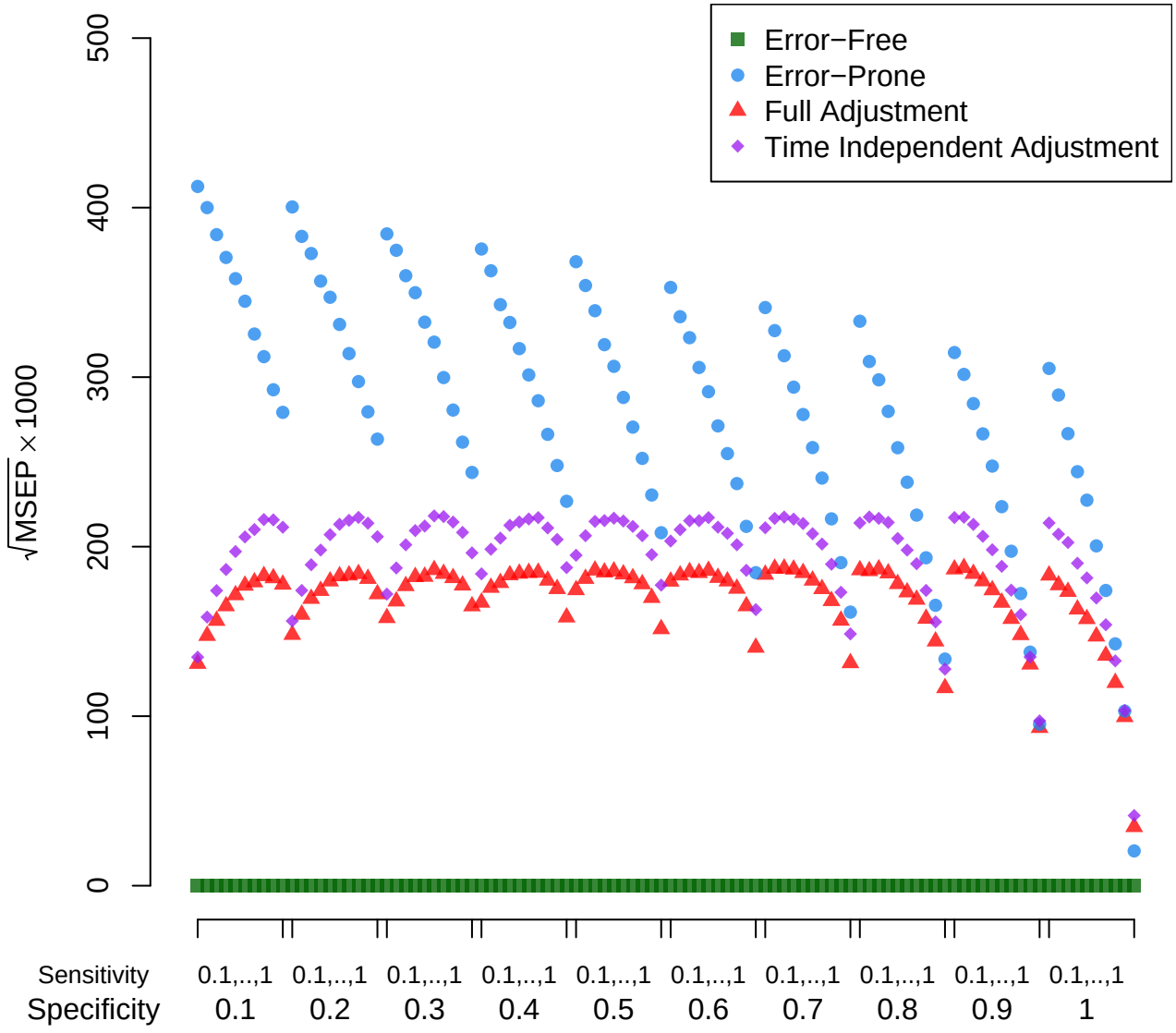

Figure 7: $\sqrt{MSEP} * 1000$ for survival simulations under varying sensitivity and specificity rates, n=200.

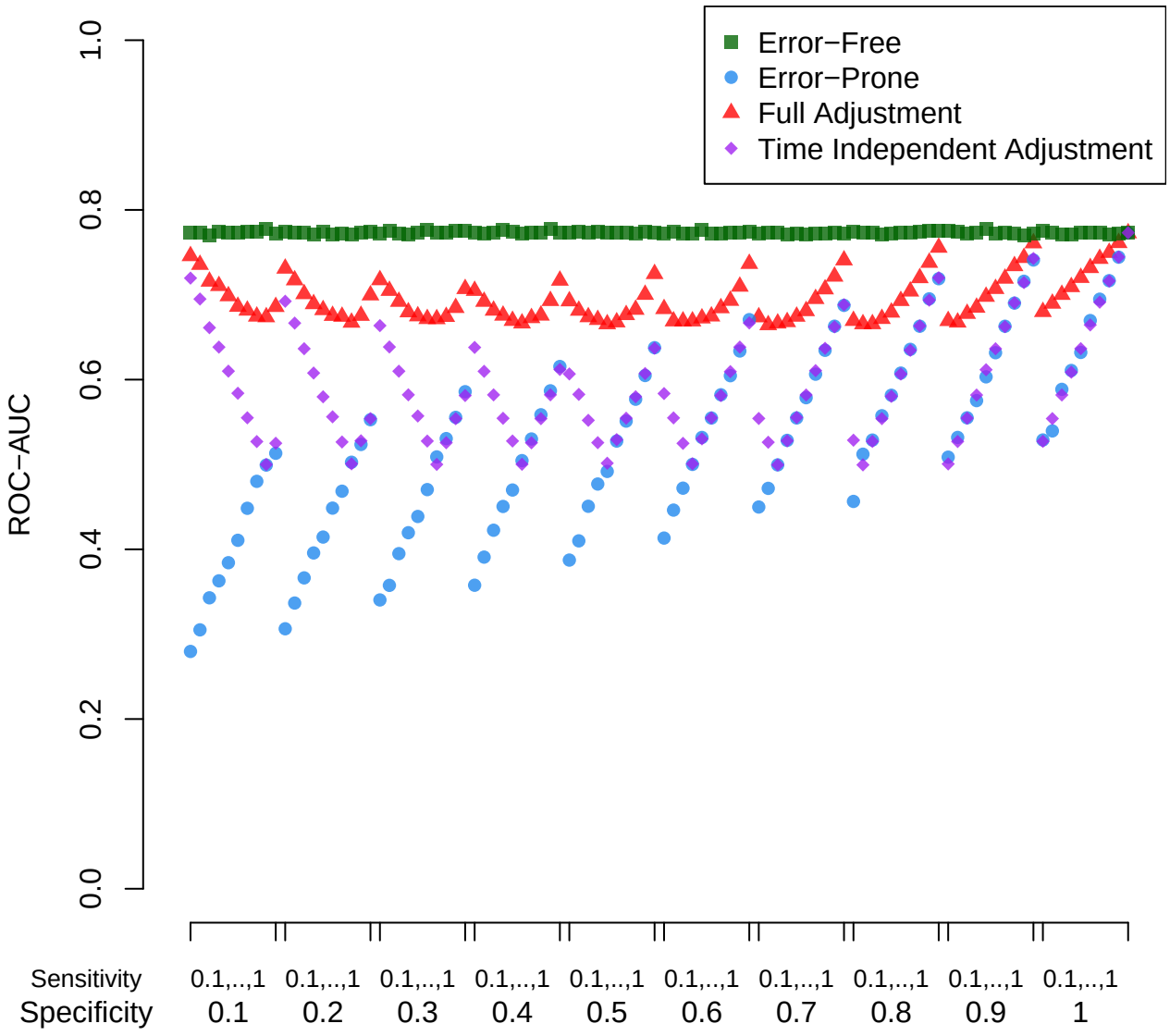

Figure 8: ROC-AUC for survival simulations under varying sensitivity and specificity rates, n=200.

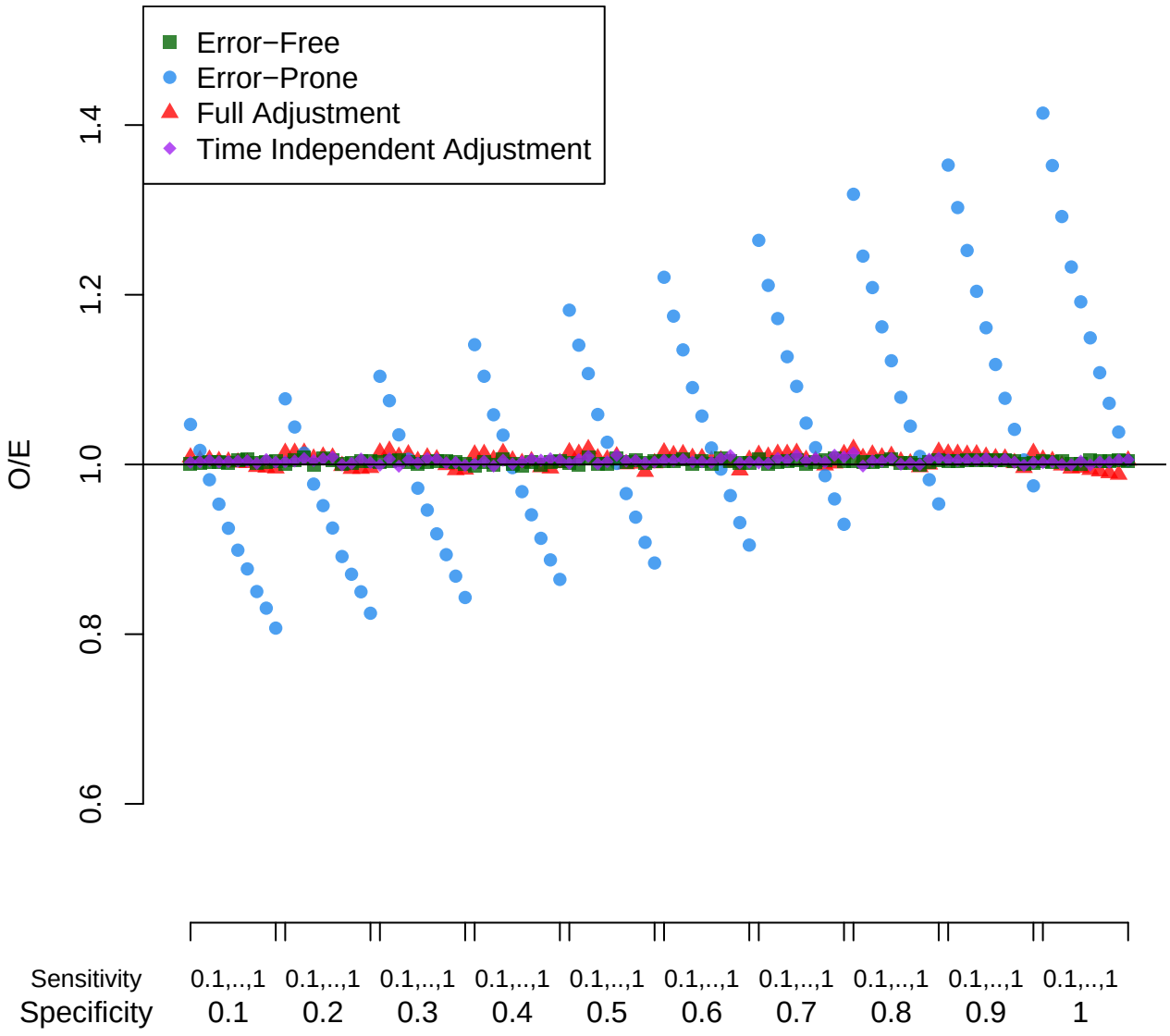

Figure 9: O/E ratios for survival simulations under varying sensitivity and specificity rates, n=400.

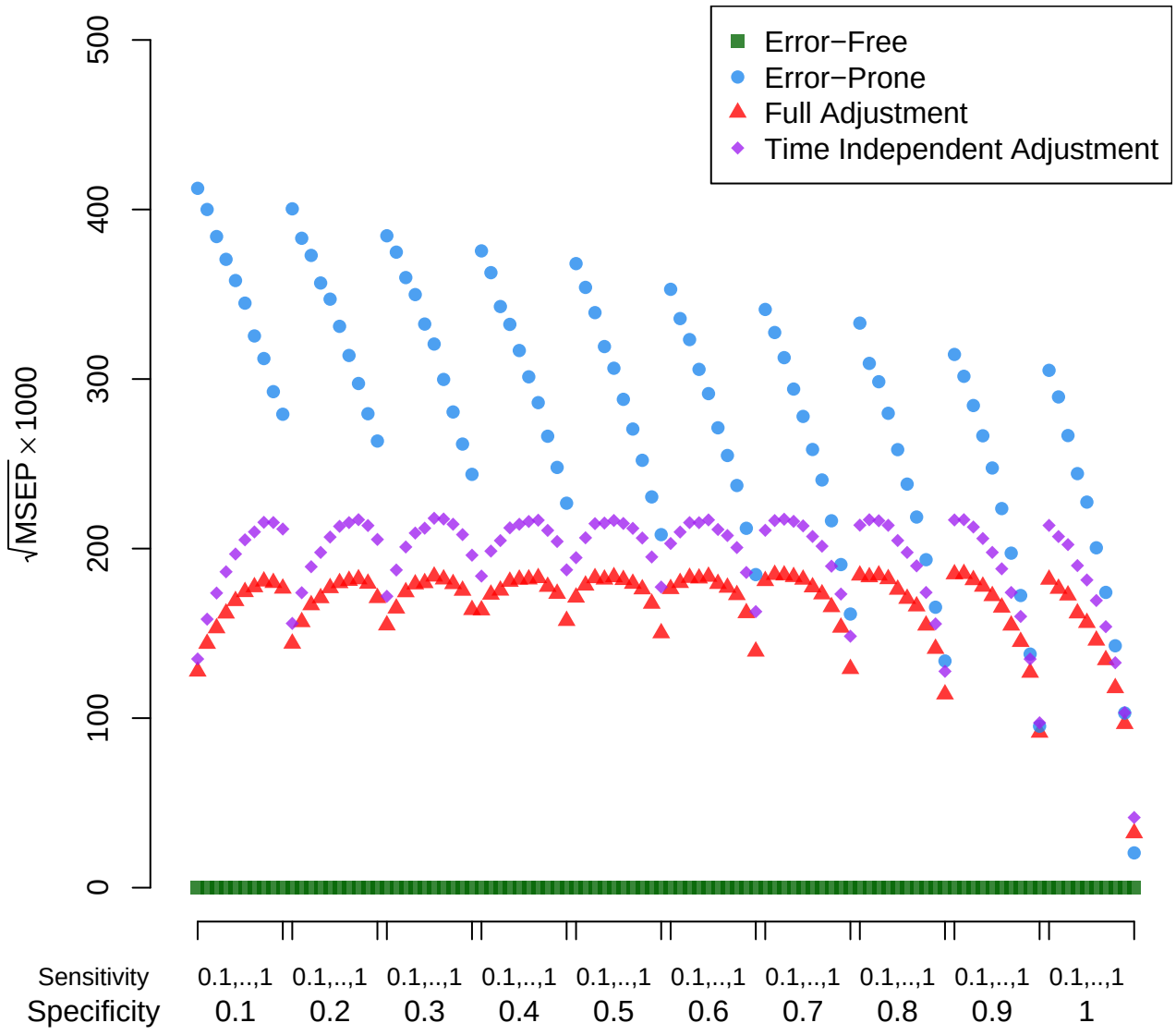

Figure 10: $\sqrt{MSEP} * 1000$ for survival simulations under varying sensitivity and specificity rates, n=400.

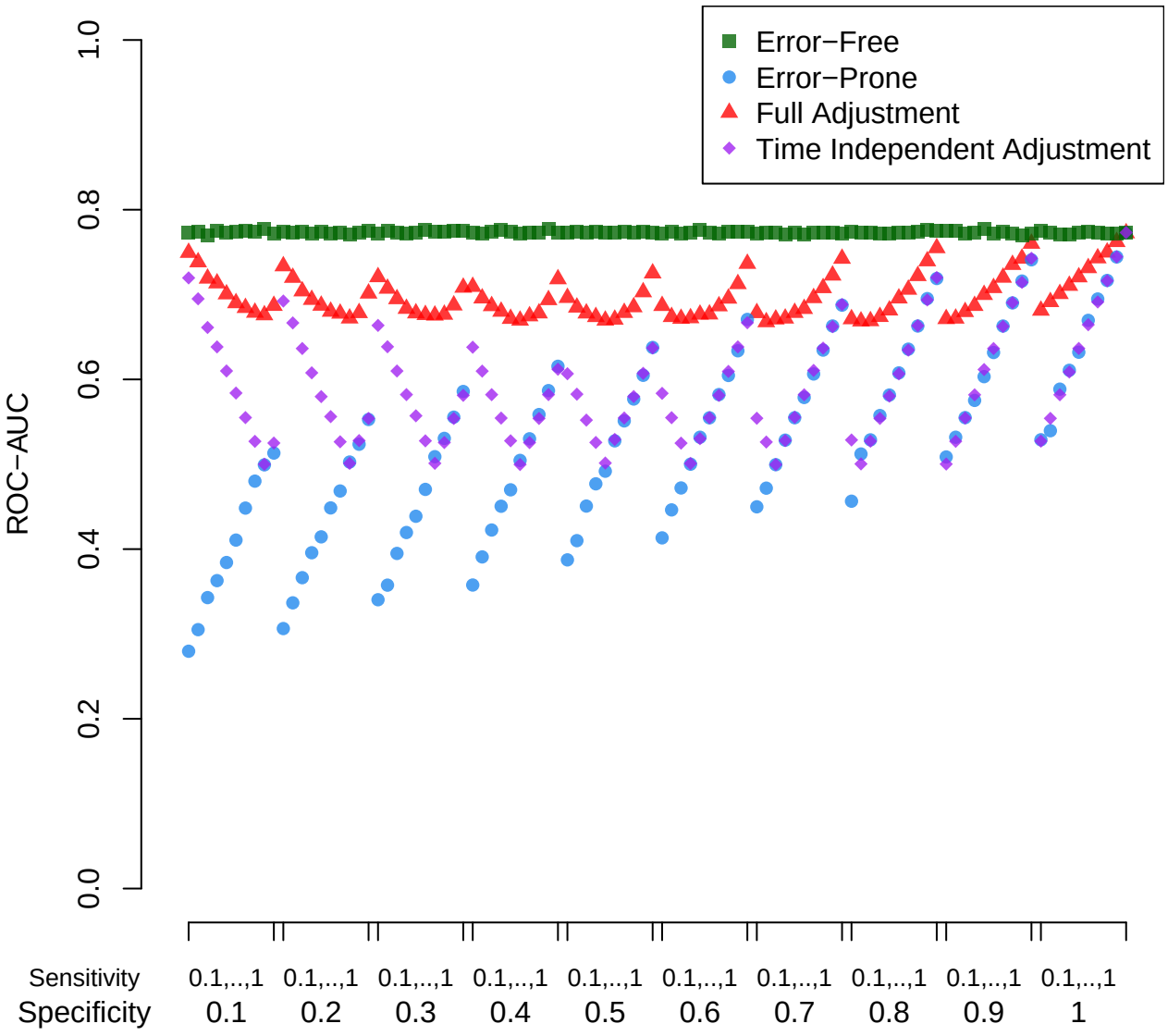

Figure 11: ROC-AUC for survival simulations under varying sensitivity and specificity rates, n=400.

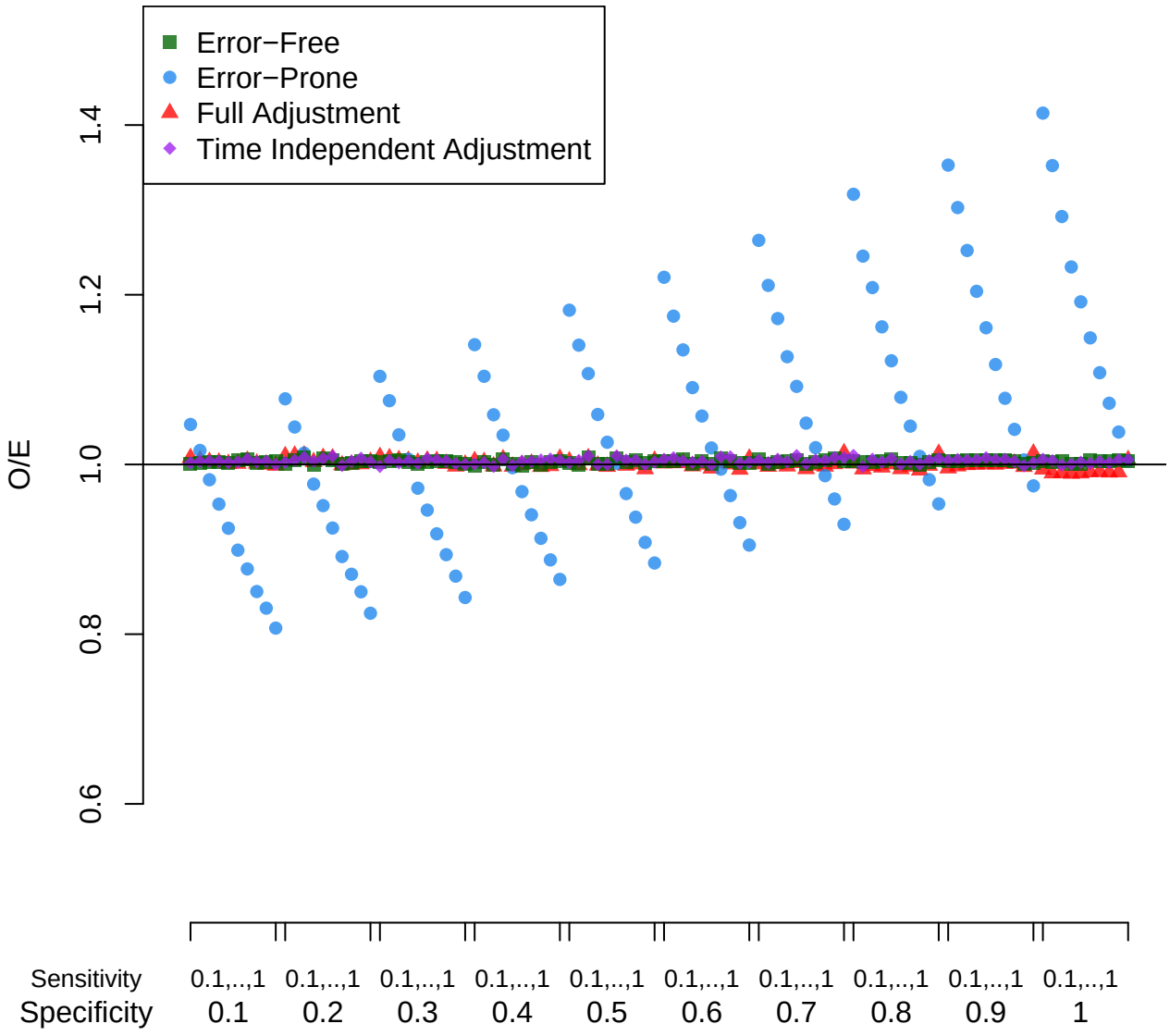

Figure 12: O/E ratios for survival simulations under varying sensitivity and specificity rates, n=800.

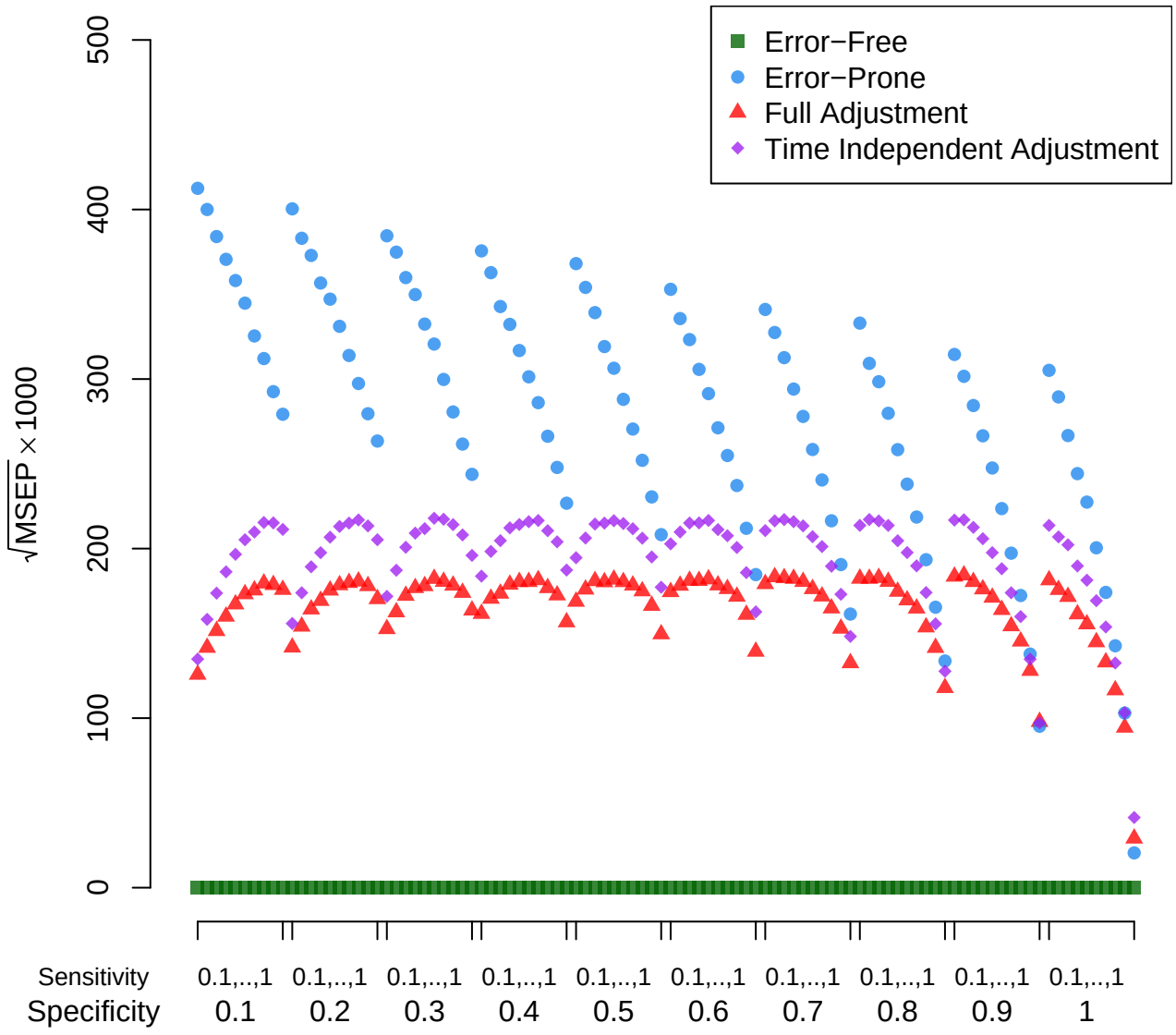

Figure 13: $\sqrt{MSEP} * 1000$ for survival simulations under varying sensitivity and specificity rates, n=800.

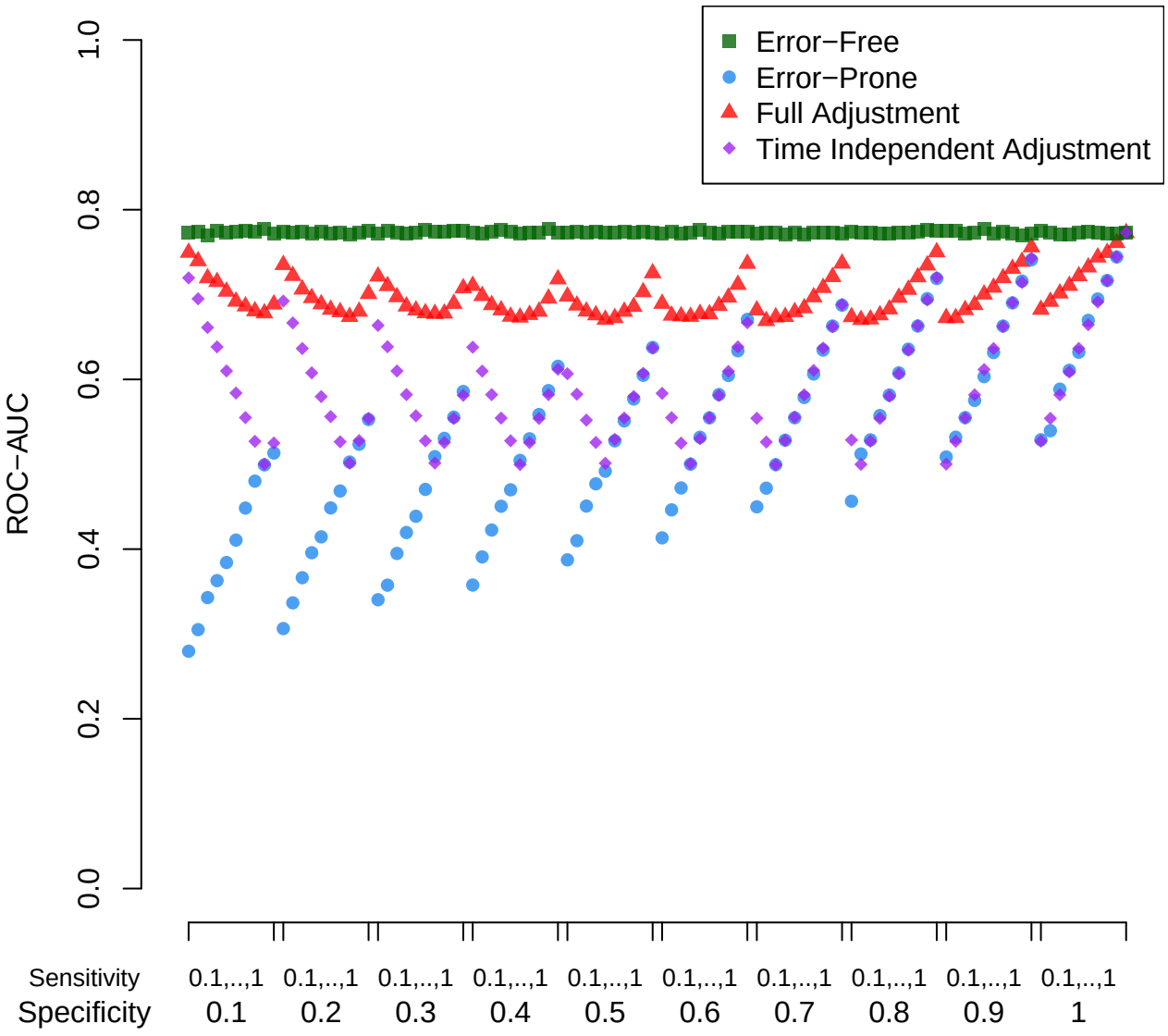

Figure 14: ROC-AUC for survival simulations under varying sensitivity and specificity rates, n=800.

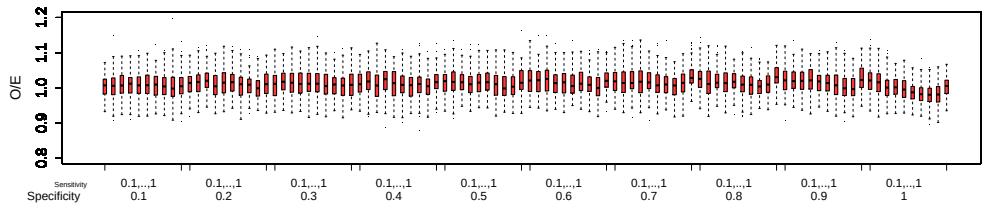

Figure 15: O/E ratios for survival simulations under varying sensitivity and specificity rates, n=100, proposed adjustment across 100 iterations.

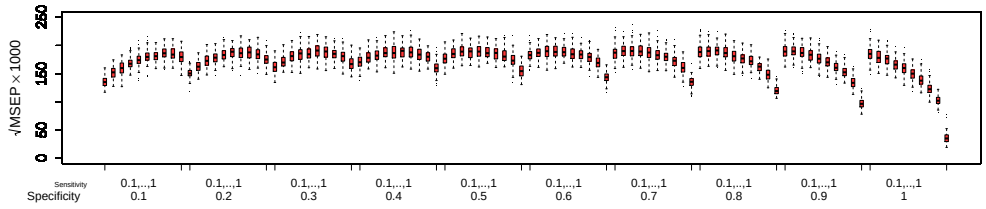

Figure 16: $\sqrt{MSEP} * 1000$ for survival simulations under varying sensitivity and specificity rates, n=100, proposed adjustment across 100 iterations.

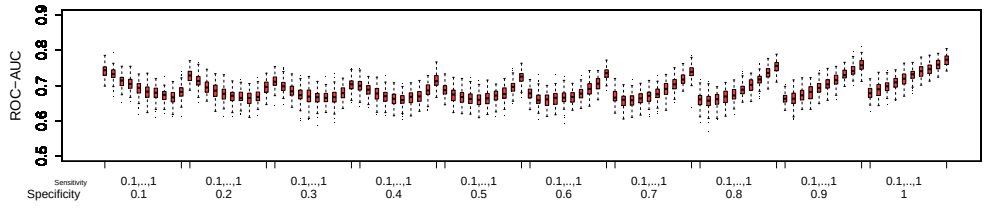

Figure 17: ROC-AUC for survival simulations under varying sensitivity and specificity rates, n=100, proposed adjustment across 100 iterations.

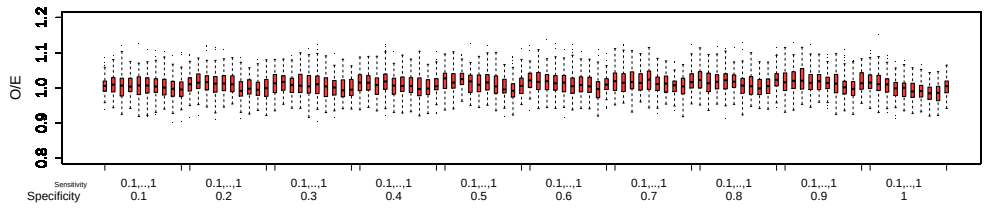

Figure 18: O/E ratios for survival simulations under varying sensitivity and specificity rates, n=200, proposed adjustment across 100 iterations.

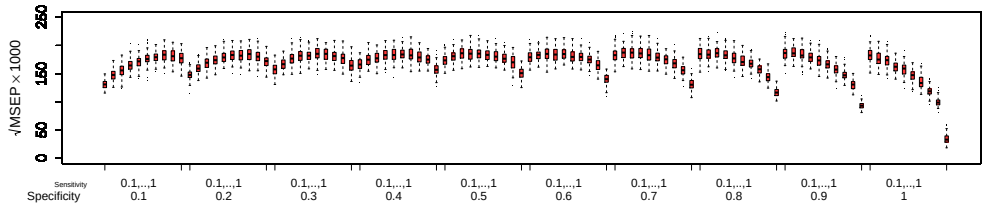

Figure 19: $\sqrt{MSEP} * 1000$ for survival simulations under varying sensitivity and specificity rates, n=200, proposed adjustment across 100 iterations.

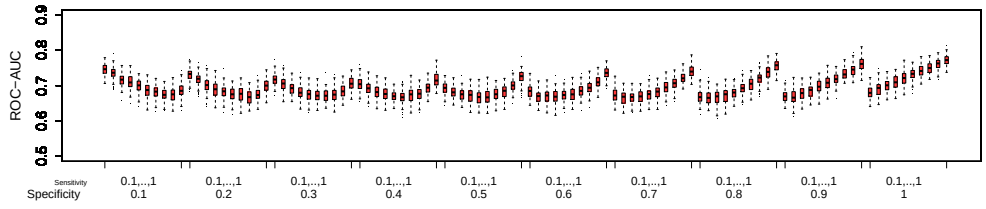

Figure 20: ROC-AUC for survival simulations under varying sensitivity and specificity rates, n=200, proposed adjustment across 100 iterations.

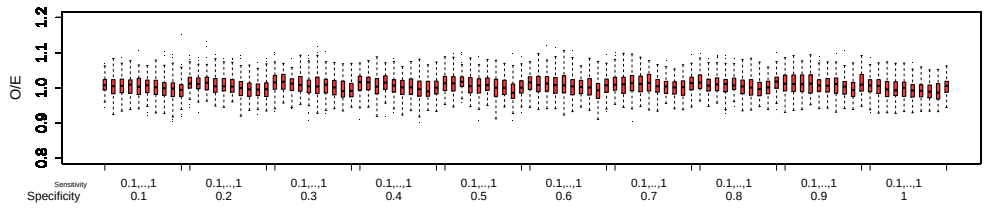

Figure 21: O/E ratios for survival simulations under varying sensitivity and specificity rates, n=400, proposed adjustment across 100 iterations.

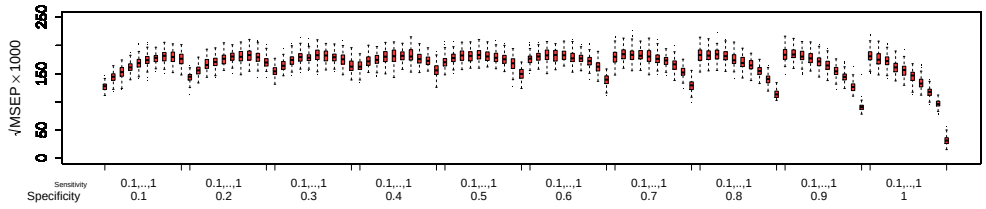

Figure 22: $\sqrt{MSEP} * 1000$ for survival simulations under varying sensitivity and specificity rates, n=400, proposed adjustment across 100 iterations.

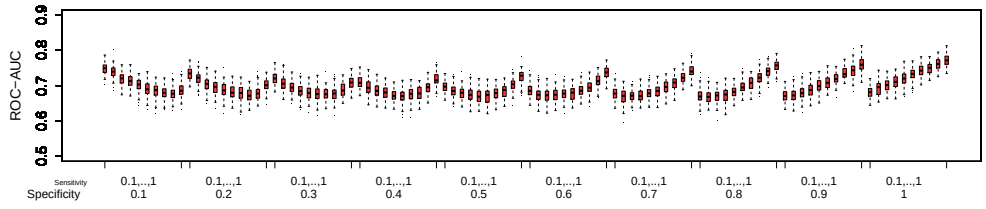

Figure 23: ROC-AUC for survival simulations under varying sensitivity and specificity rates, n=400, proposed adjustment across 100 iterations.

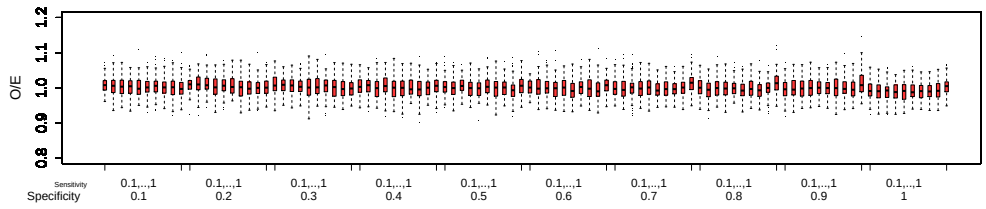

Figure 24: O/E ratios for survival simulations under varying sensitivity and specificity rates, n=800, proposed adjustment across 100 iterations.

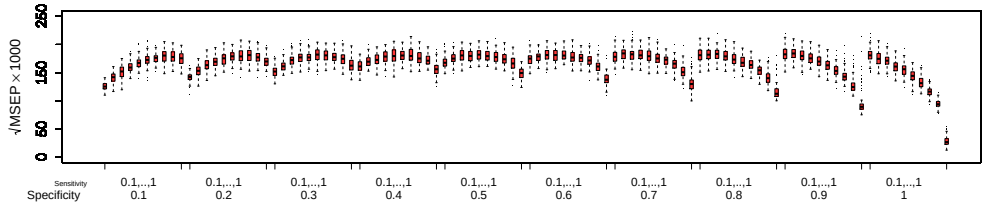

Figure 25: $\sqrt{MSEP} * 1000$ for survival simulations under varying sensitivity and specificity rates, n=800, proposed adjustment across 100 iterations.

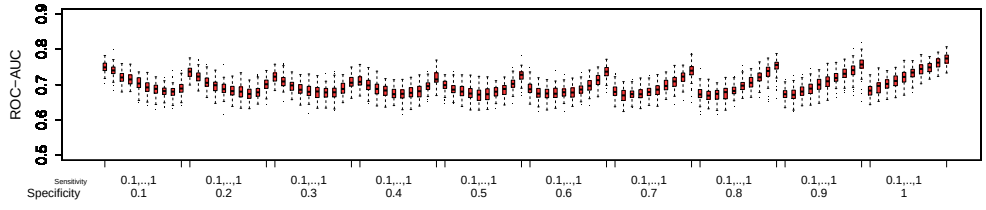

Figure 26: ROC-AUC for survival simulations under varying sensitivity and specificity rates, n=800, proposed adjustment across 100 iterations.

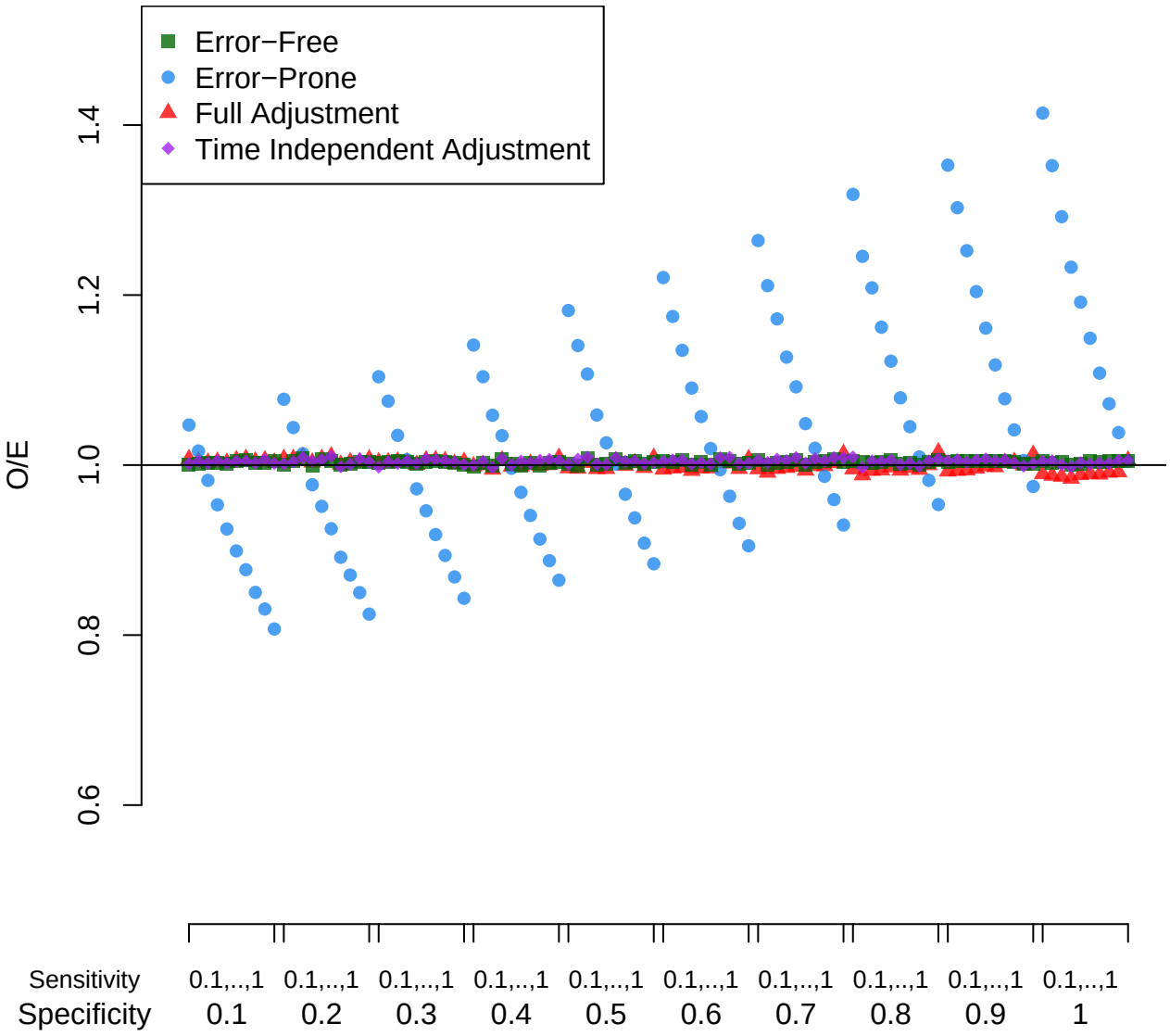

Figure 27: O/E ratios for survival simulations under varying sensitivity and specificity rates, band width=0.1, n=1000.

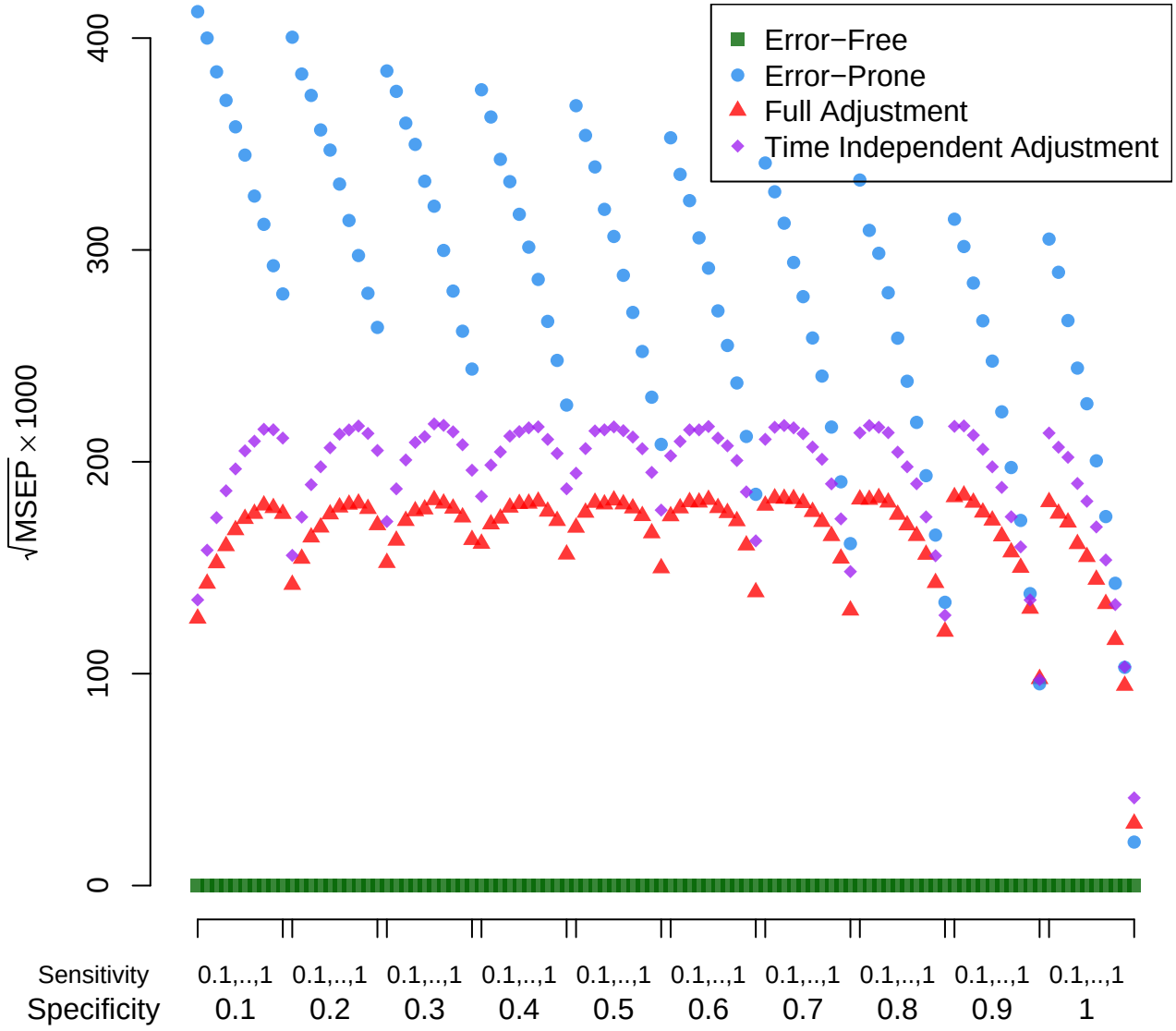

Figure 28: $\sqrt{MSEP} * 1000$ for survival simulations under varying sensitivity and specificity rates, band width=0.1, n=1000.

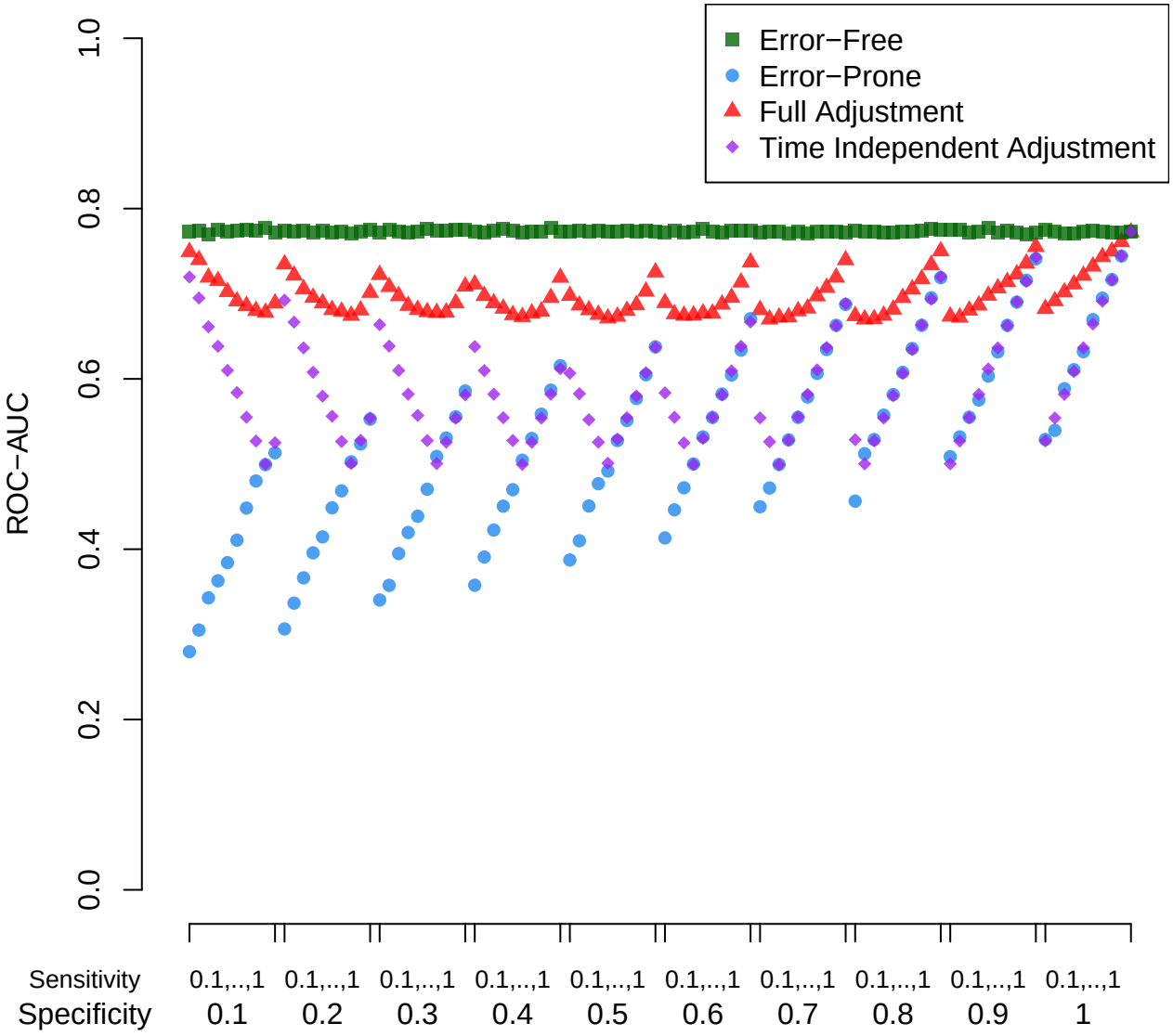

Figure 29: ROC-AUC for survival simulations under varying sensitivity and specificity rates, band width=0.1, n=1000.

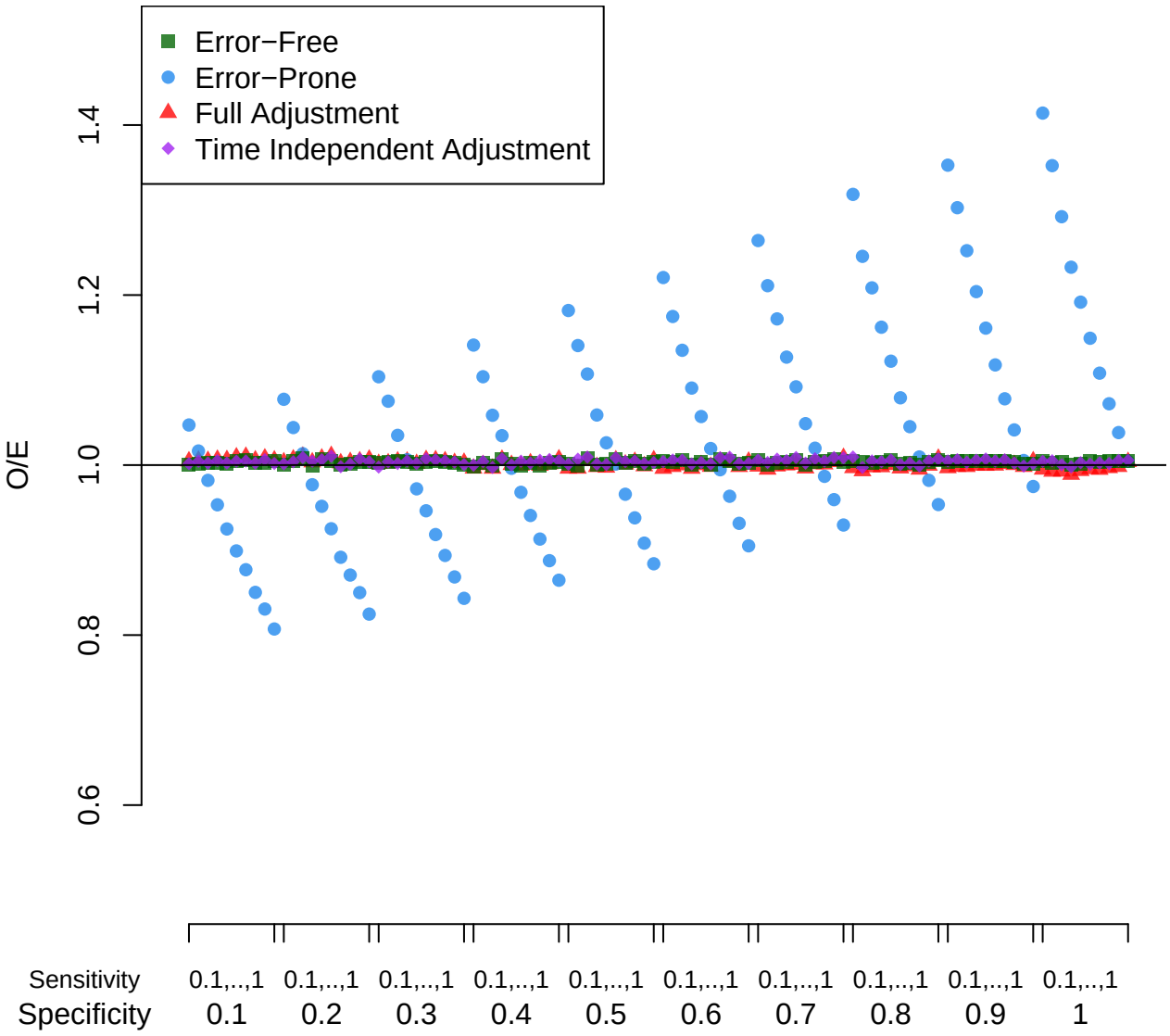

Figure 30: O/E ratios for survival simulations under varying sensitivity and specificity rates, band width=0.2, n=1000.

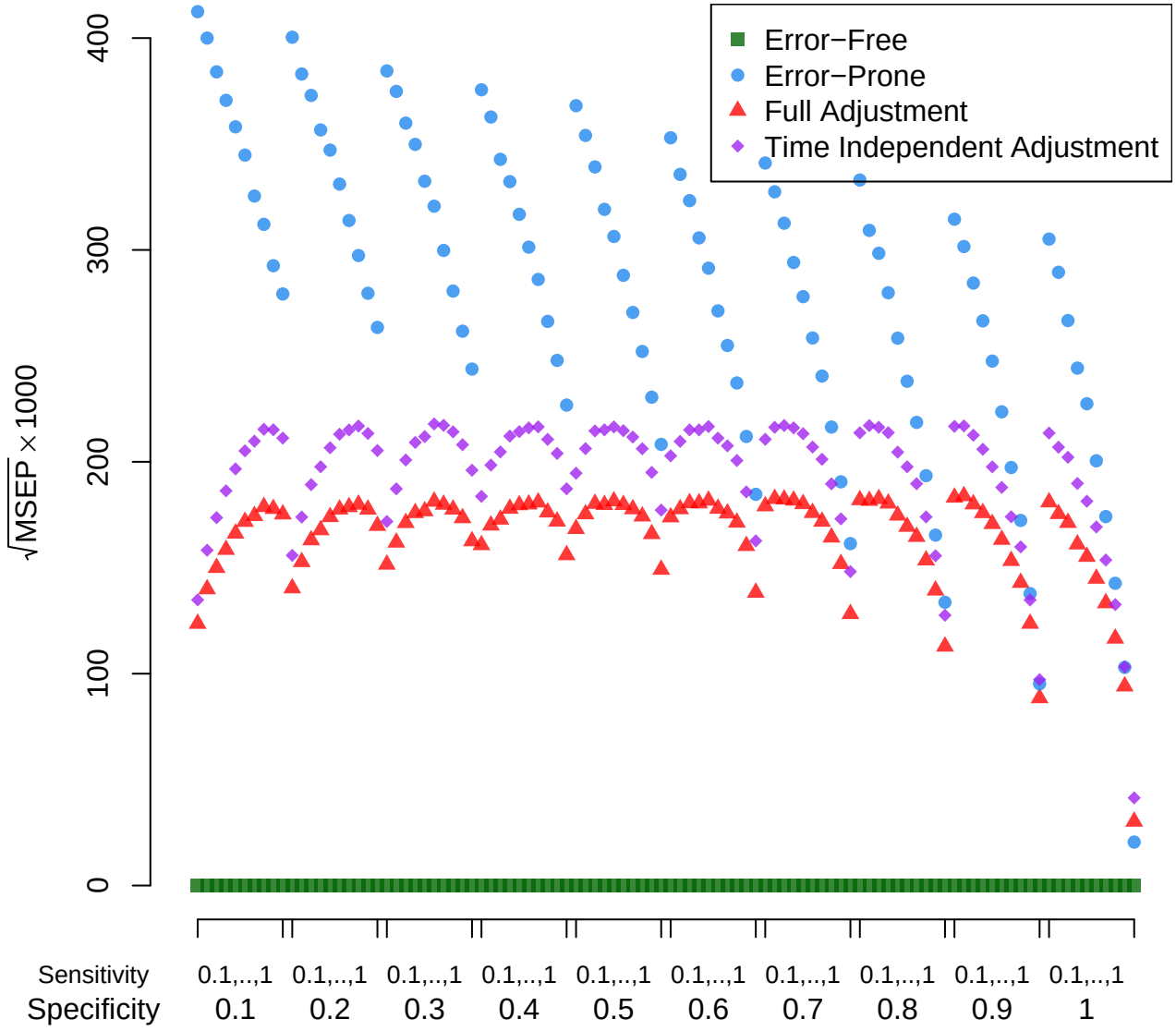

Figure 31: $\sqrt{MSEP} * 1000$ for survival simulations under varying sensitivity and specificity rates, band width=0.2, n=1000.

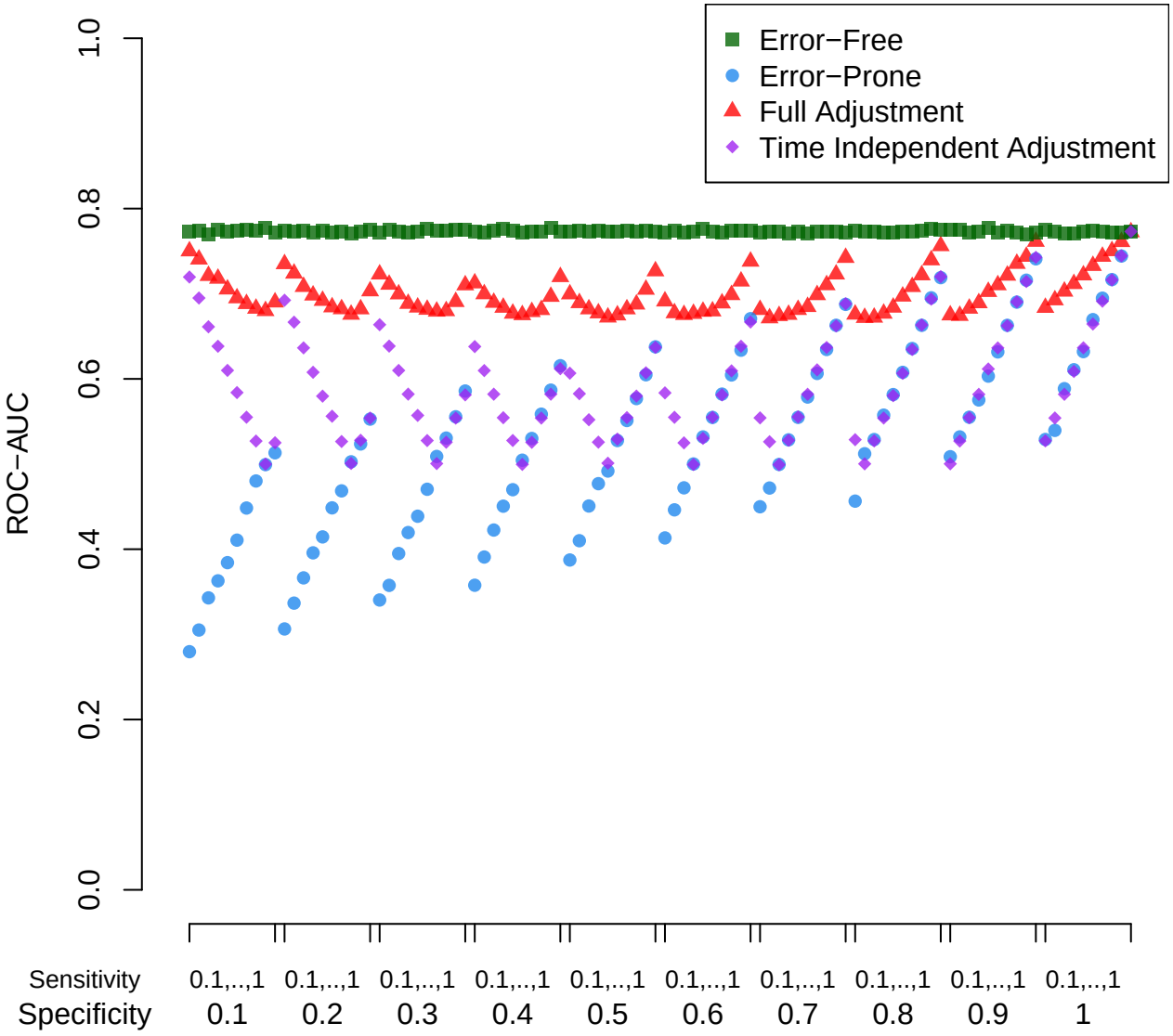

Figure 32: ROC-AUC for survival simulations under varying sensitivity and specificity rates, band width=0.2, n=1000.

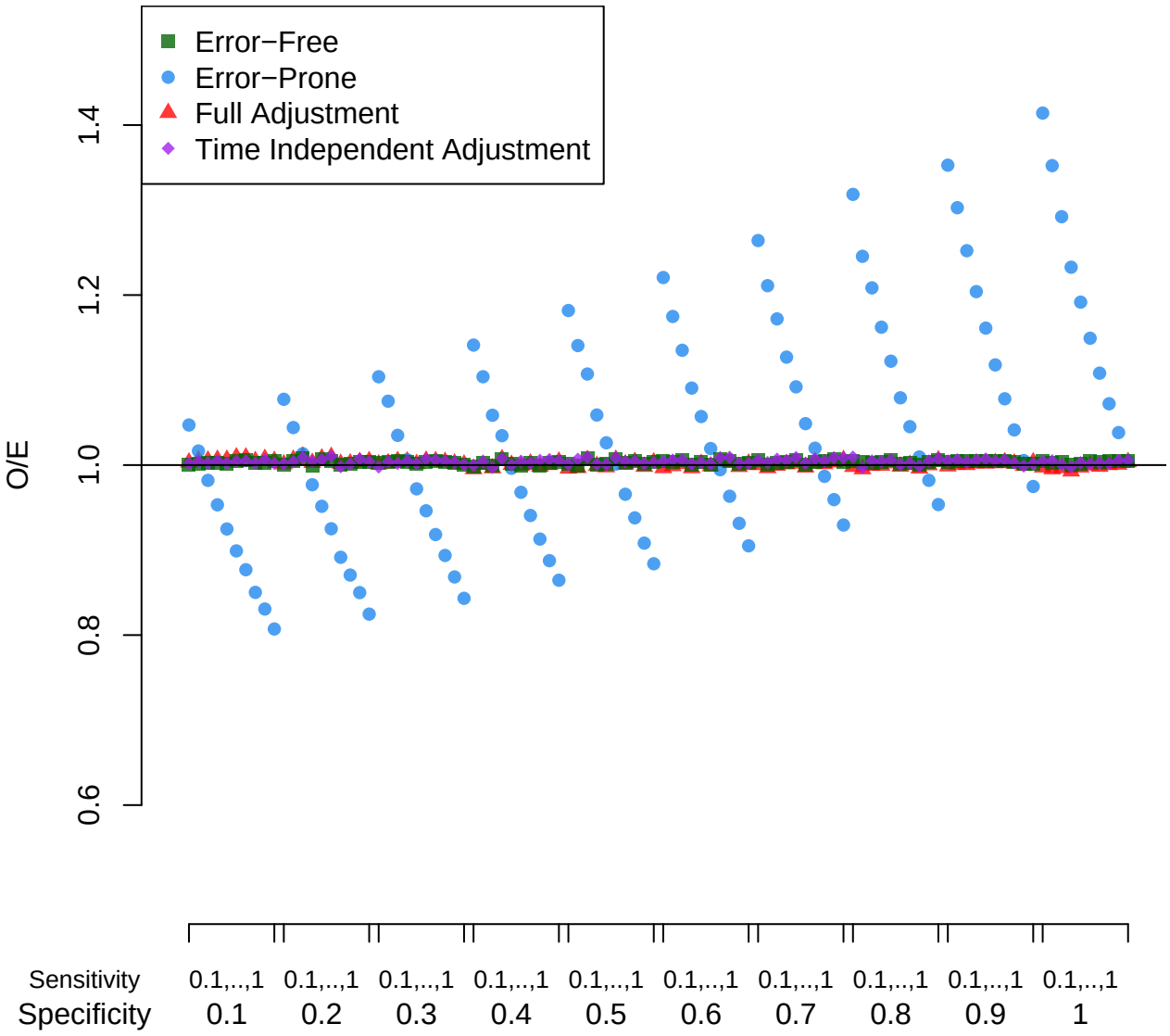

Figure 33: O/E ratios for survival simulations under varying sensitivity and specificity rates, band width=0.3, n=1000.

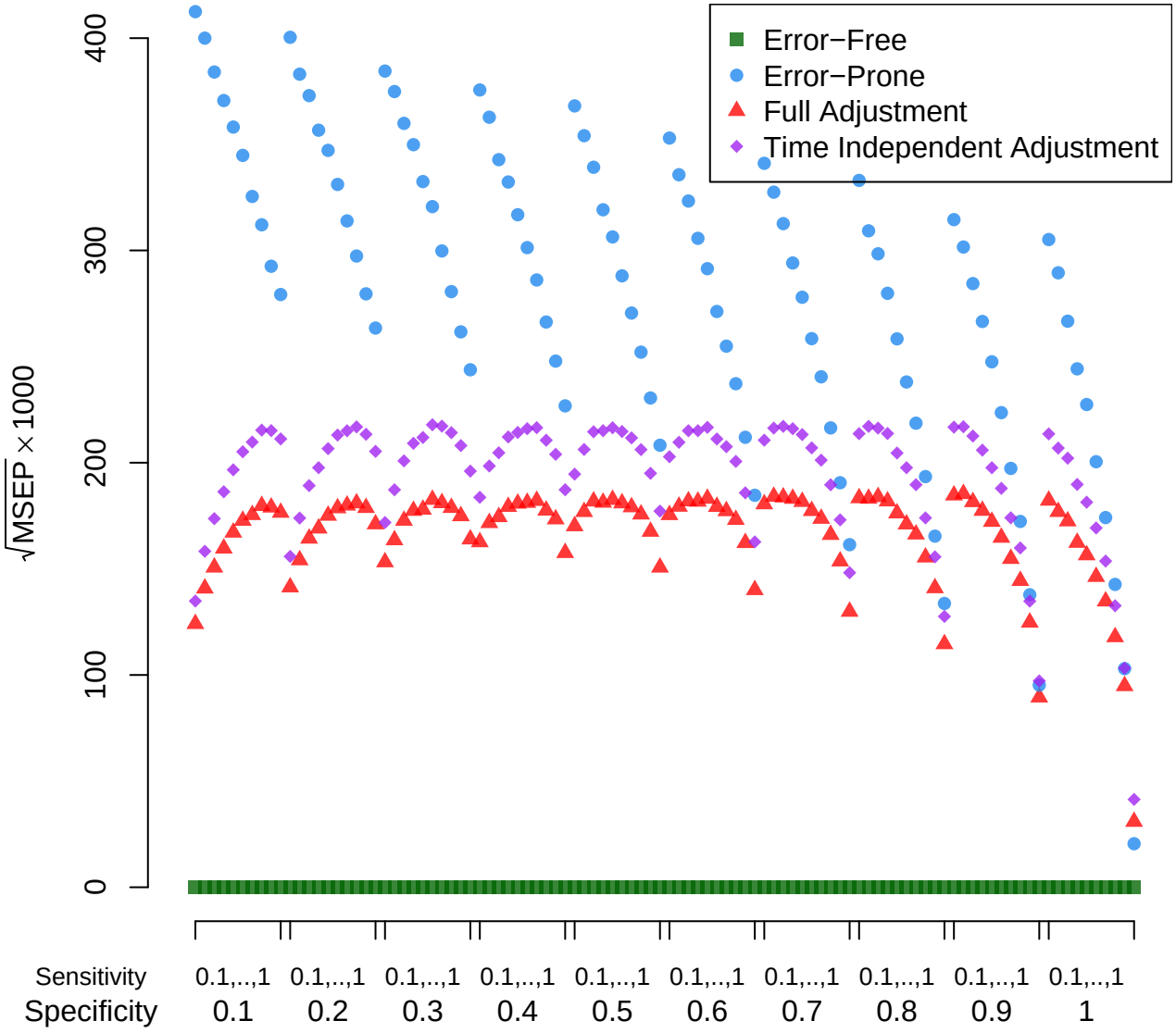

Figure 34: $\sqrt{MSEP} * 1000$ for survival simulations under varying sensitivity and specificity rates, band width=0.3, n=1000.

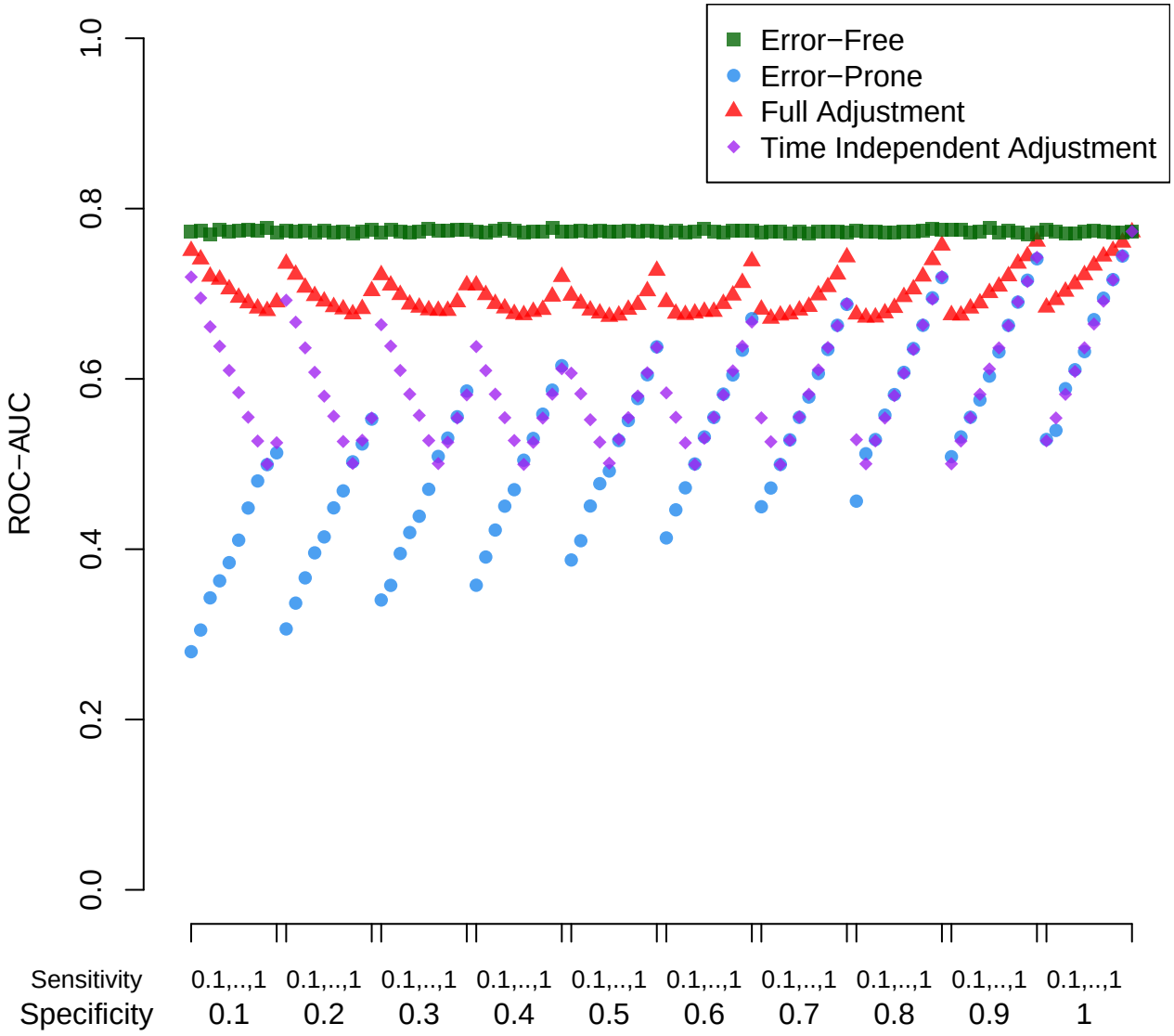

Figure 35: ROC-AUC for survival simulations under varying sensitivity and specificity rates, band width=0.3, n=1000.

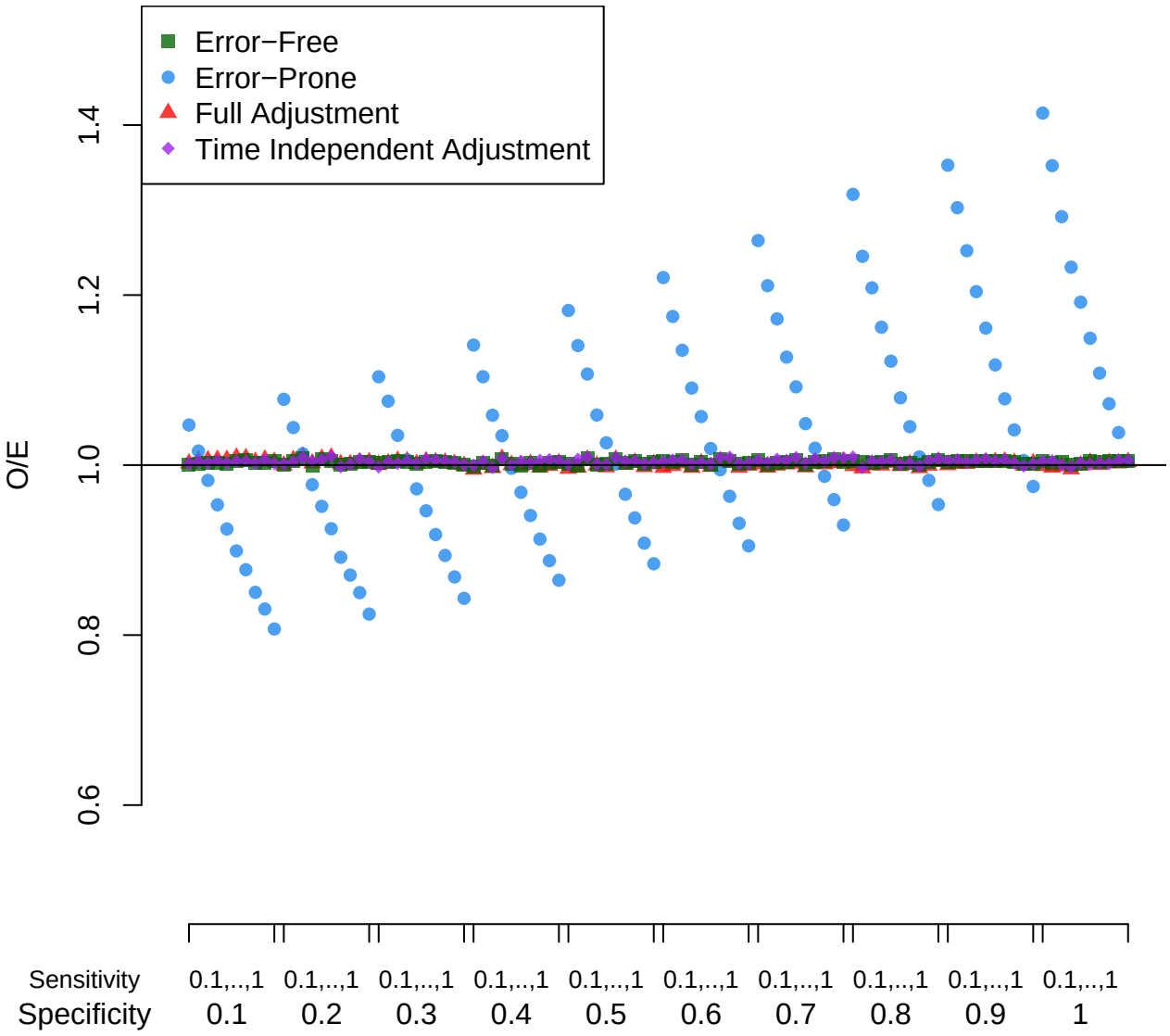

Figure 36: O/E ratios for survival simulations under varying sensitivity and specificity rates, band width=0.4, n=1000.

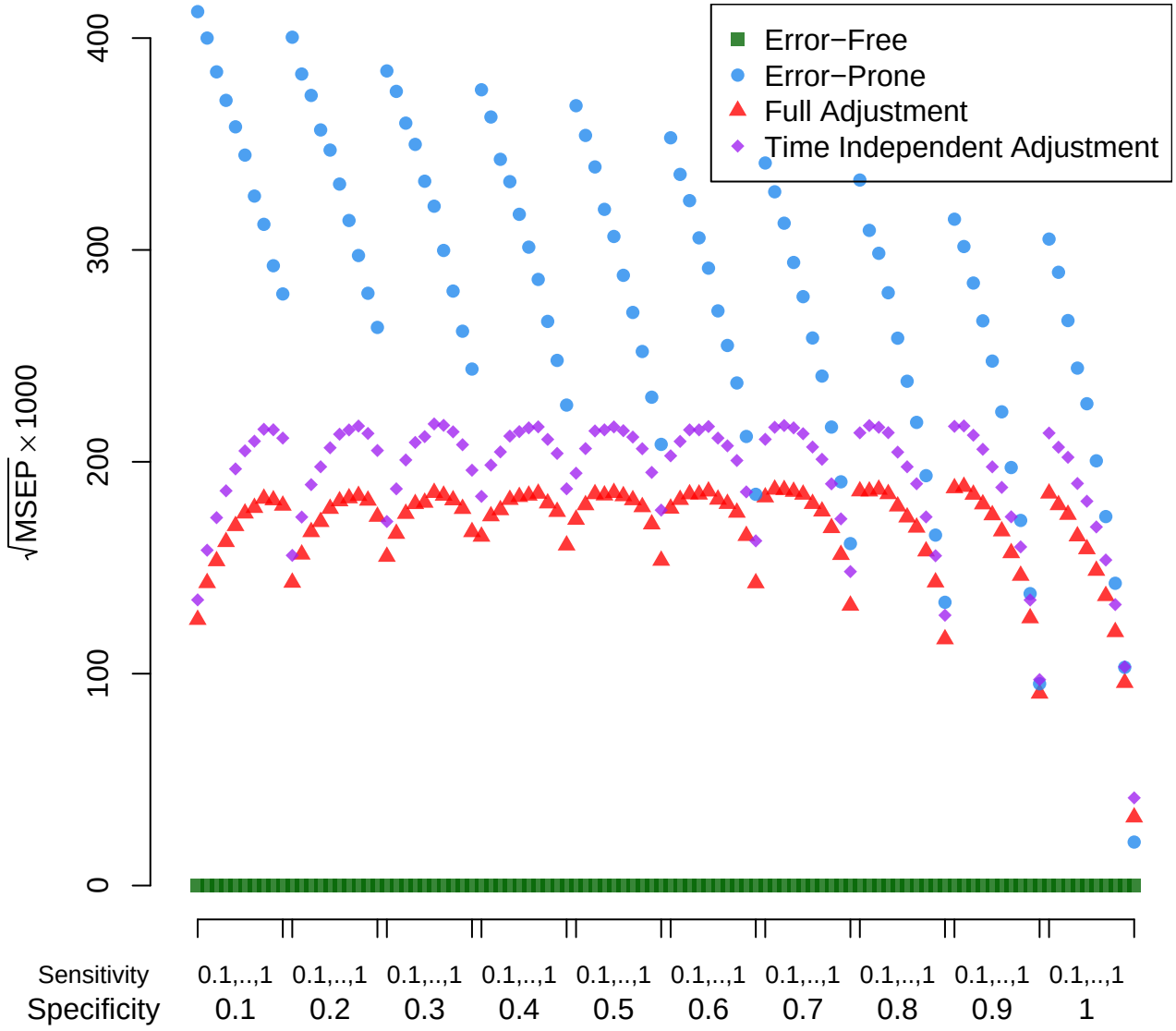

Figure 37: $\sqrt{MSEP} * 1000$ for survival simulations under varying sensitivity and specificity rates, band width=0.4, n=1000.

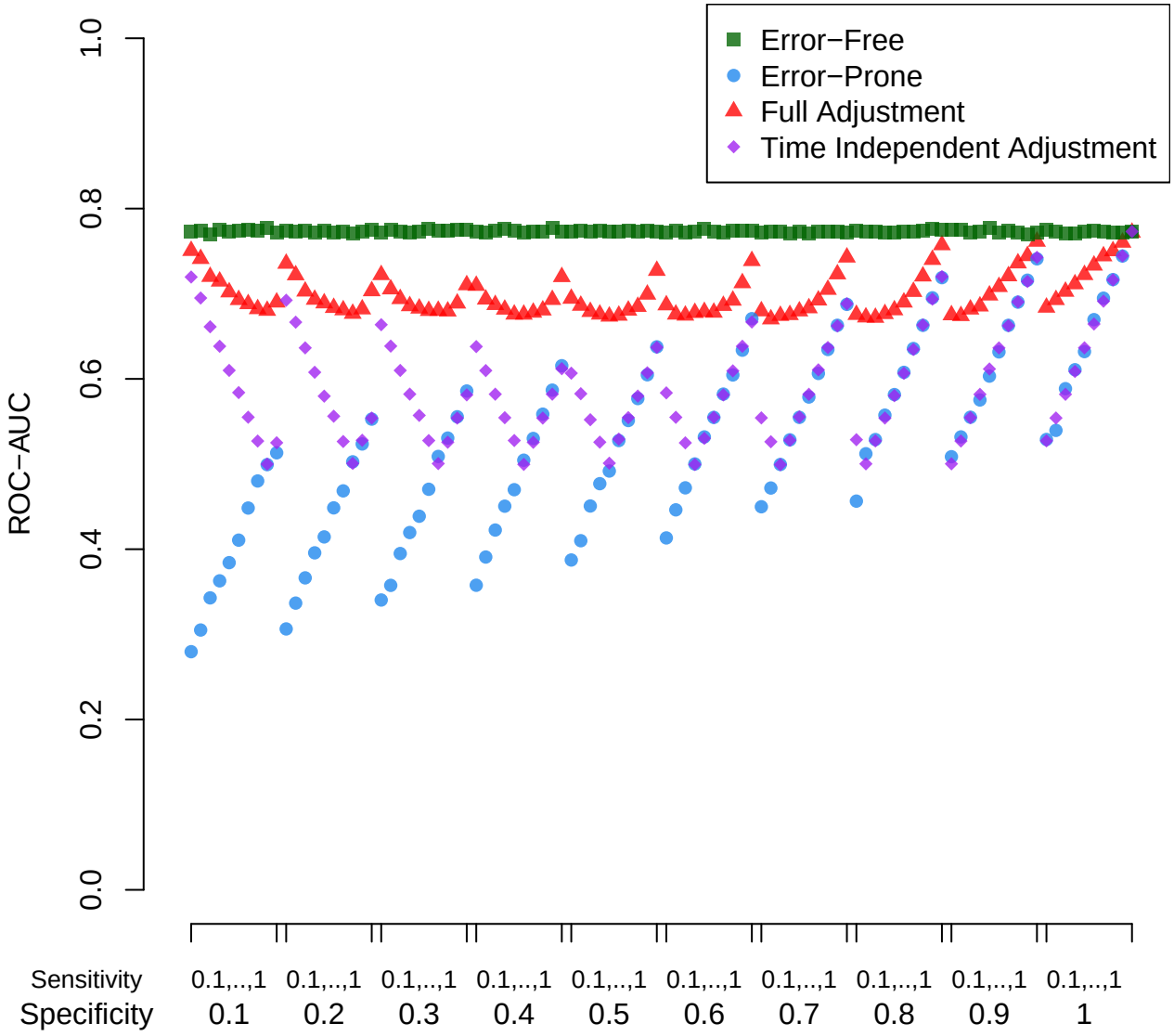

Figure 38: ROC-AUC for survival simulations under varying sensitivity and specificity rates, band width=0.4, n=1000.

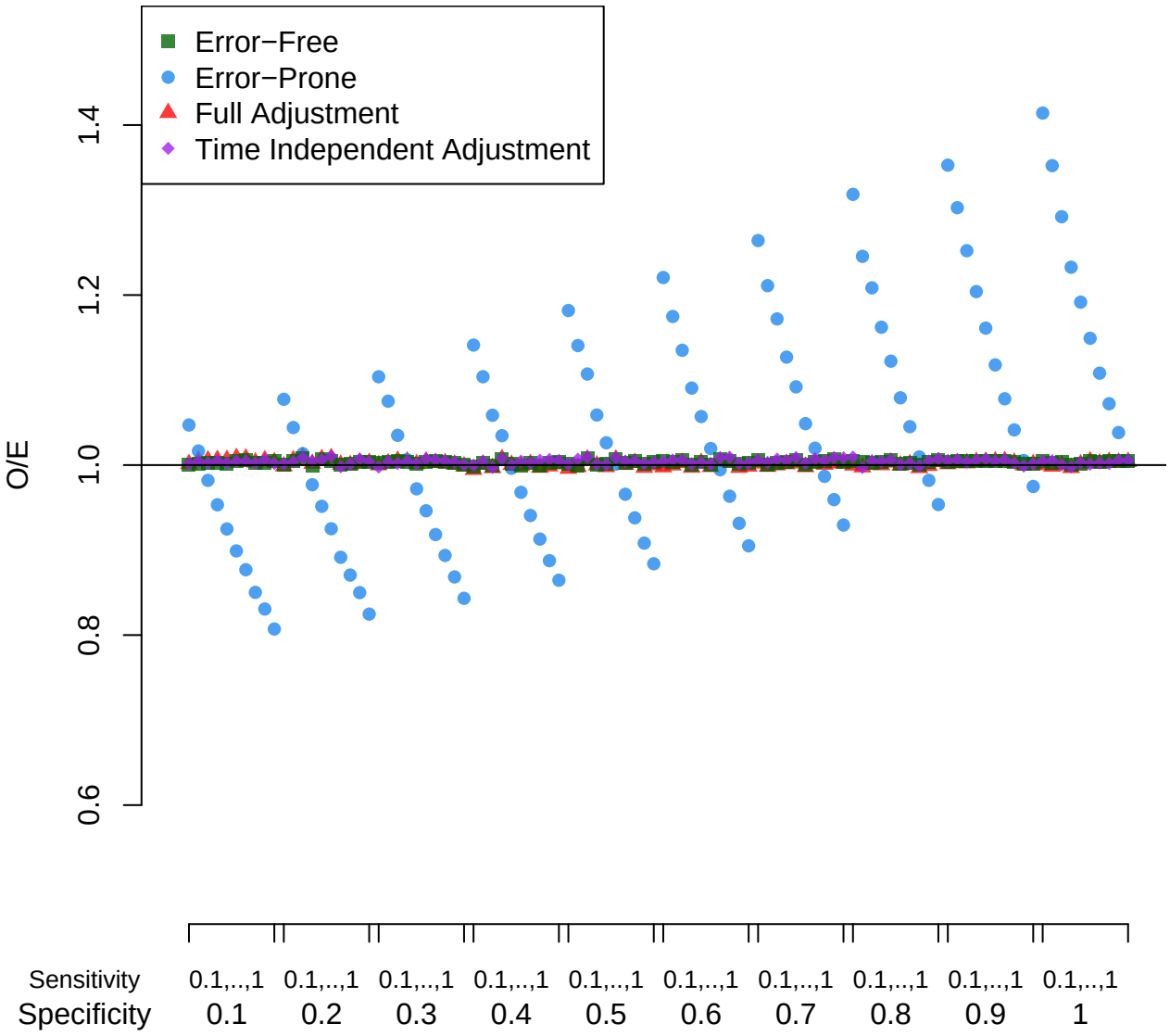

Figure 39: O/E ratios for survival simulations under varying sensitivity and specificity rates, band width=0.5, n=1000.

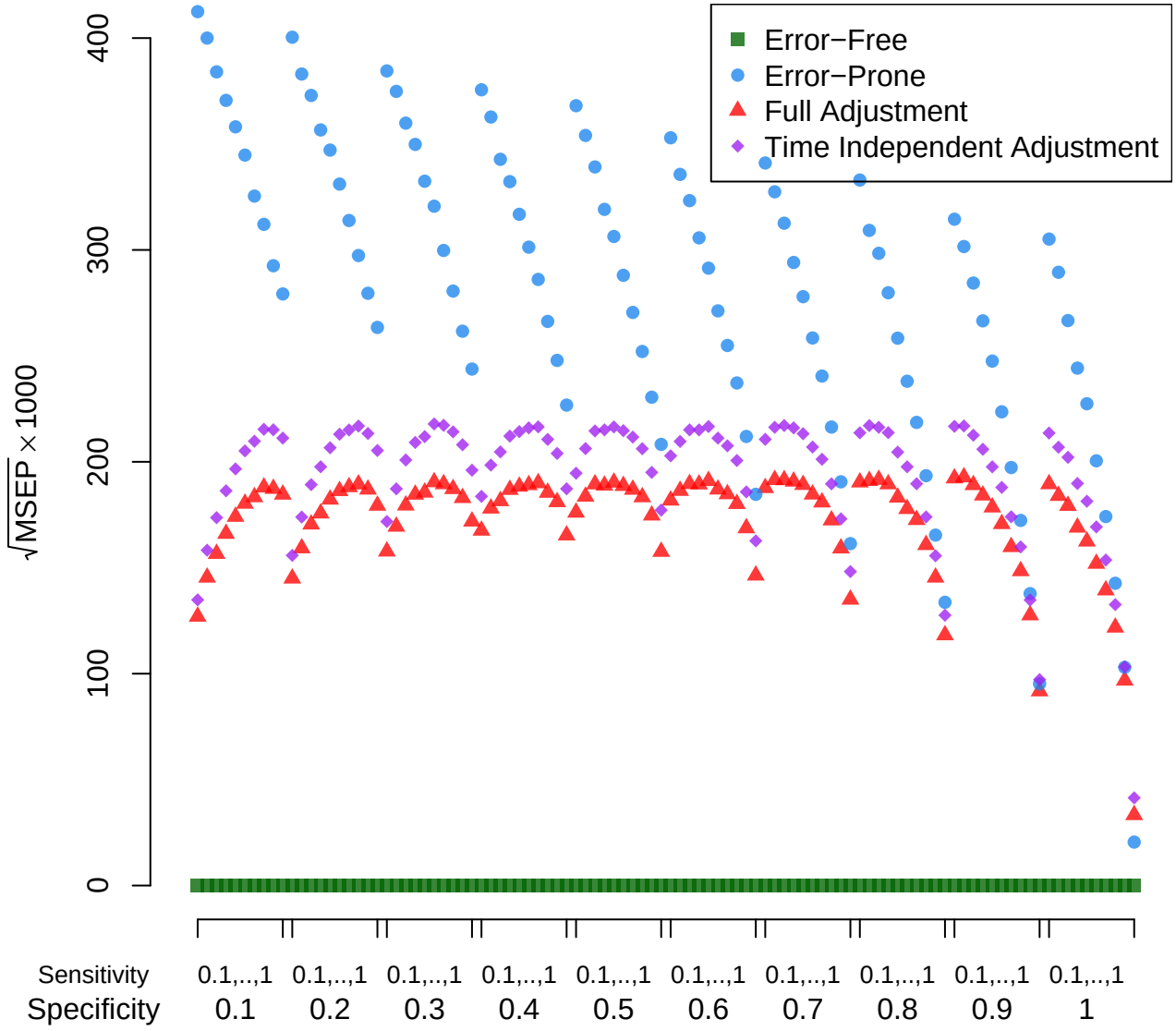

Figure 40: $\sqrt{MSEP} * 1000$ for survival simulations under varying sensitivity and specificity rates, band width=0.5, n=1000.

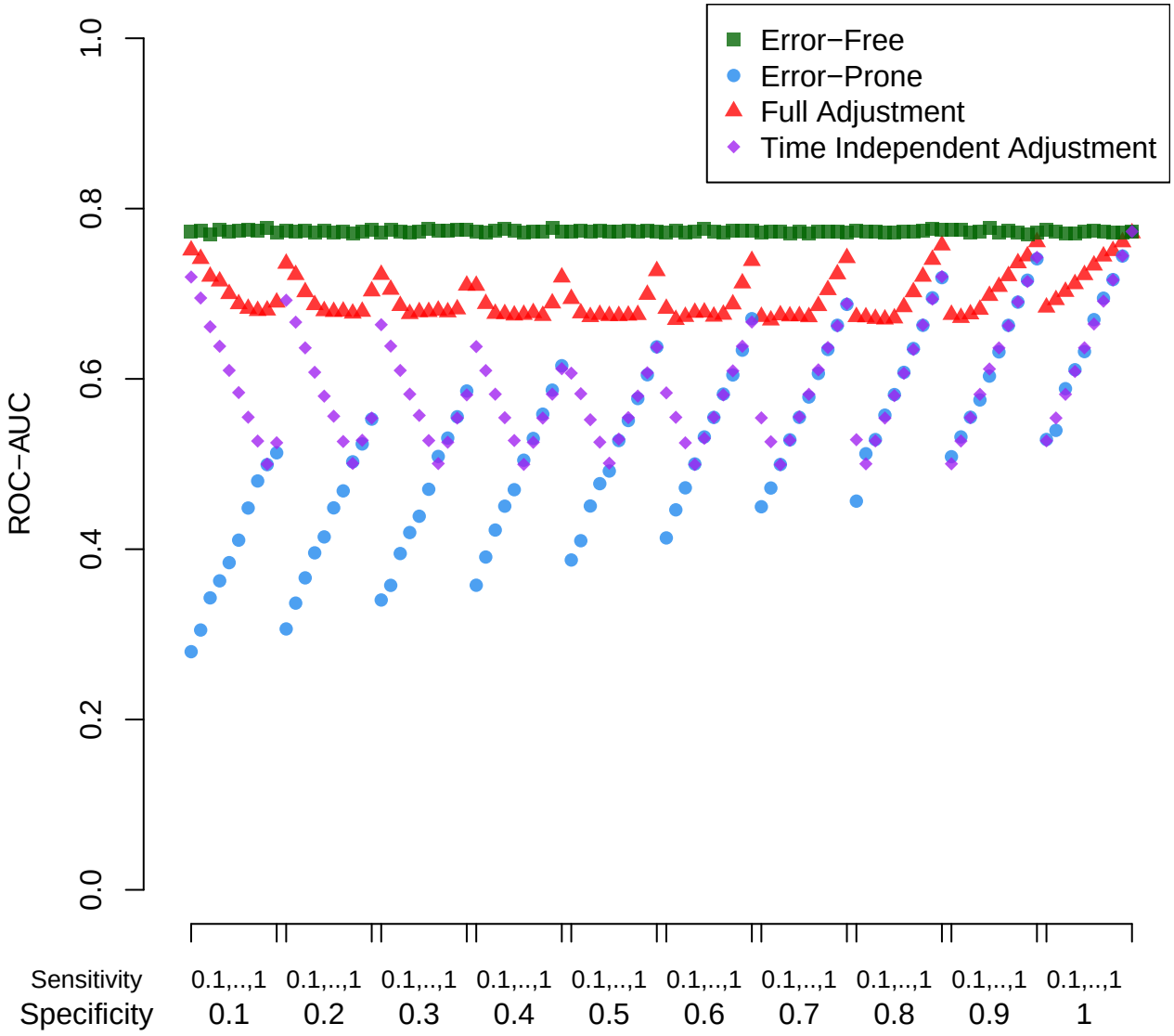

Figure 41: ROC-AUC for survival simulations under varying sensitivity and specificity rates, band width=0.5, n=1000.

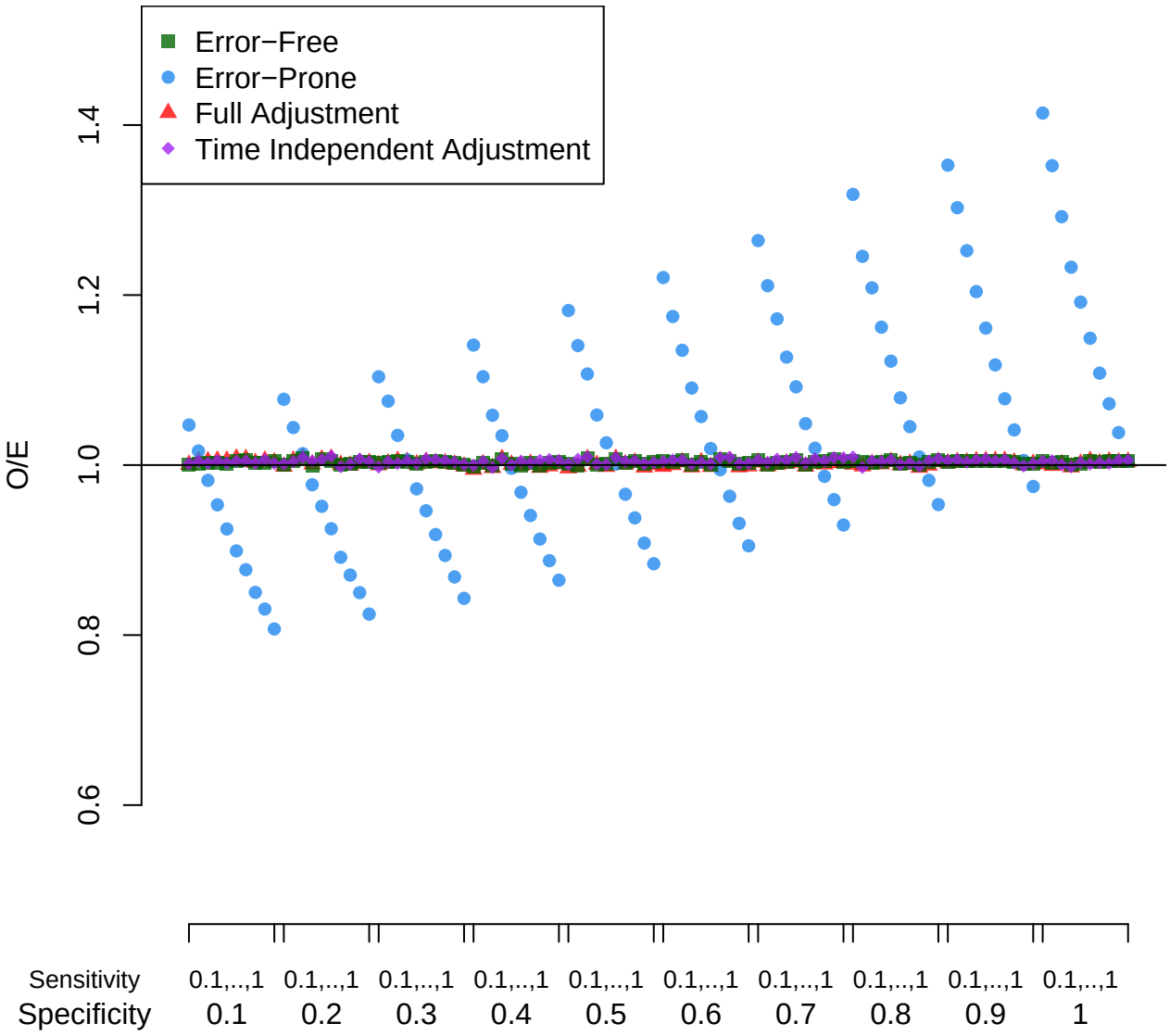

Figure 42: O/E ratios for survival simulations under varying sensitivity and specificity rates, band width=0.6, n=1000.

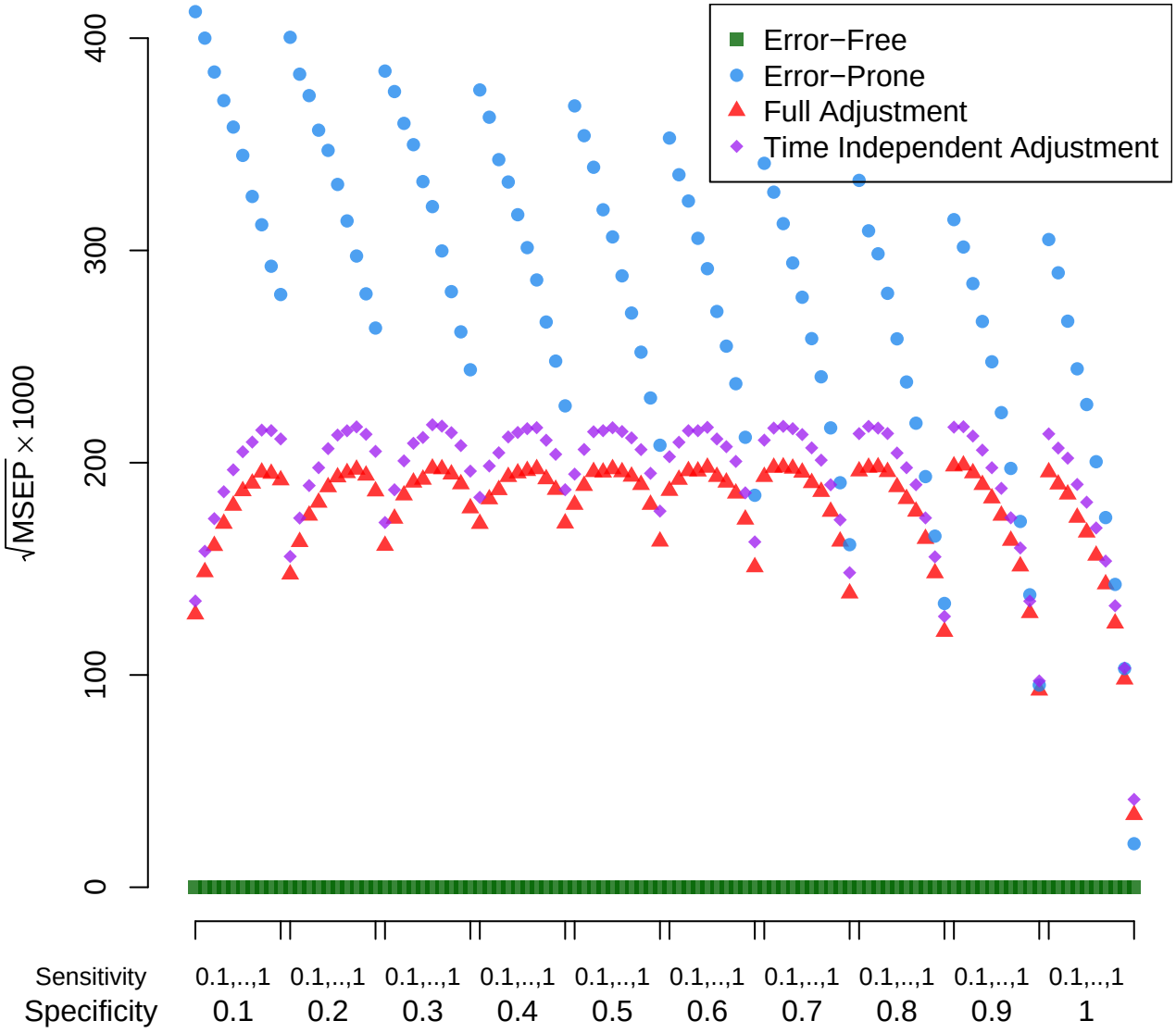

Figure 43: $\sqrt{MSEP} * 1000$ for survival simulations under varying sensitivity and specificity rates, band width=0.6, n=1000.

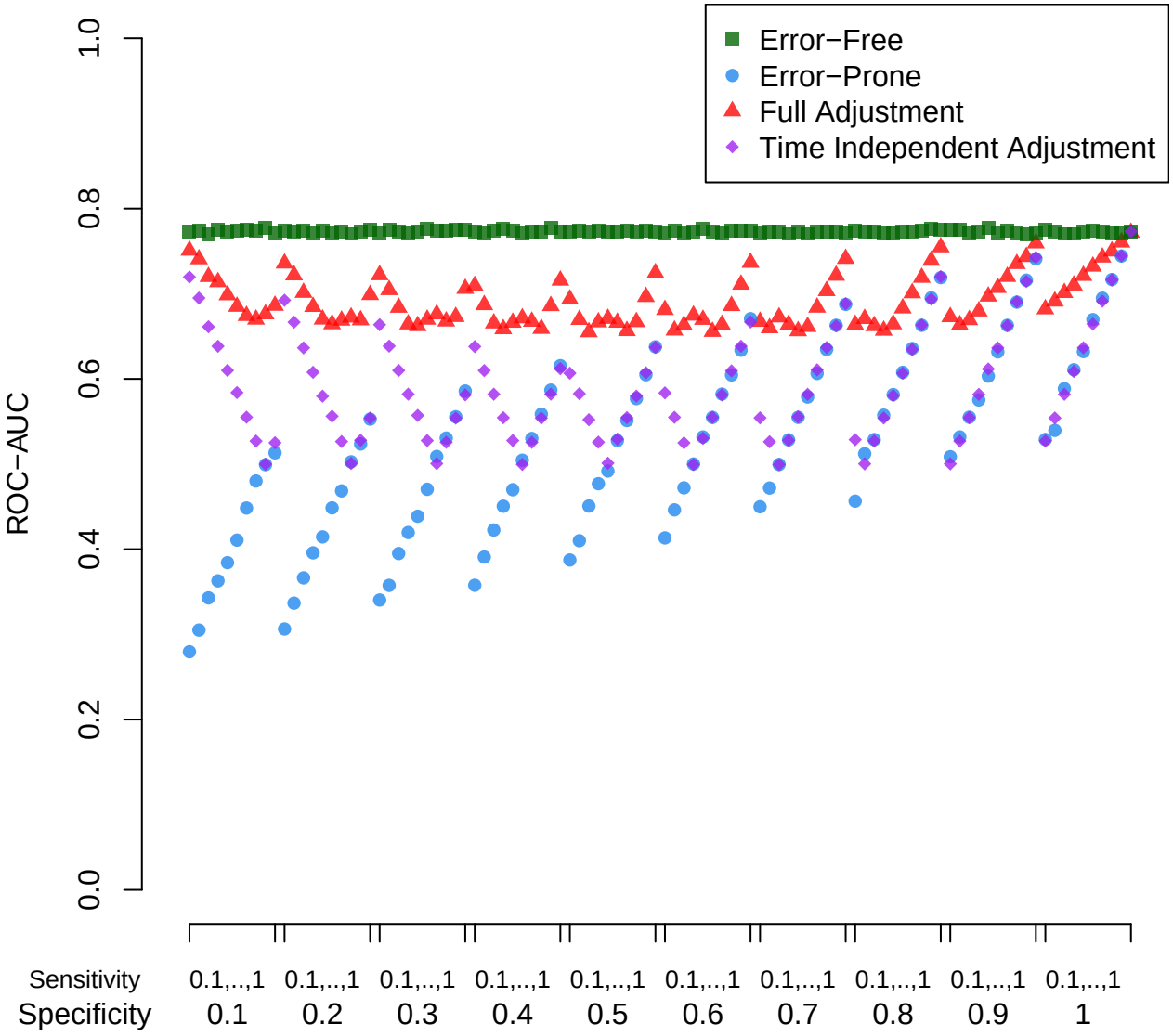

Figure 44: ROC-AUC for survival simulations under varying sensitivity and specificity rates, band width=0.6, n=1000.

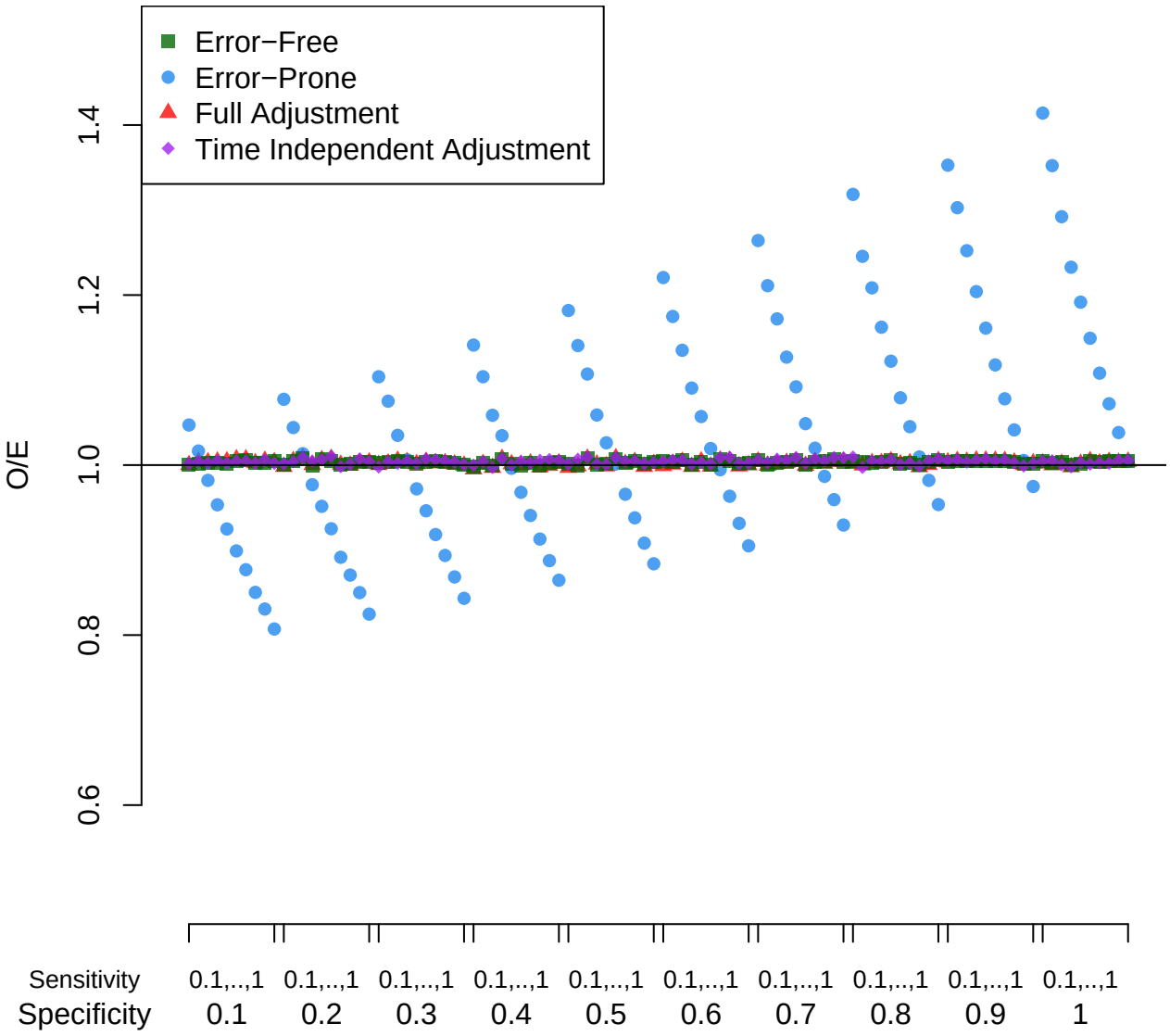

Figure 45: O/E ratios for survival simulations under varying sensitivity and specificity rates, band width=0.7, n=1000.

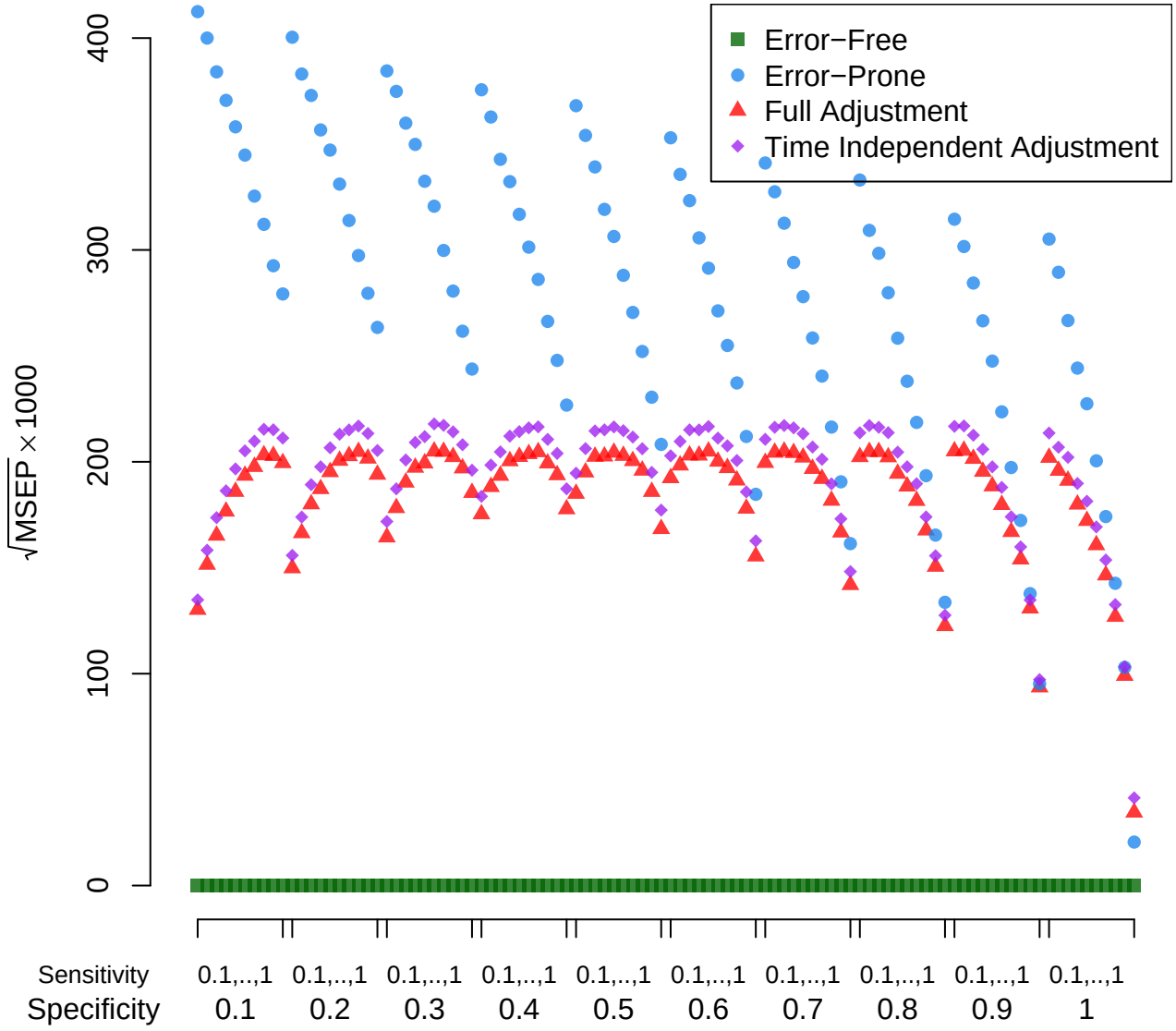

Figure 46: $\sqrt{MSEP} * 1000$ for survival simulations under varying sensitivity and specificity rates, band width=0.7, n=1000.

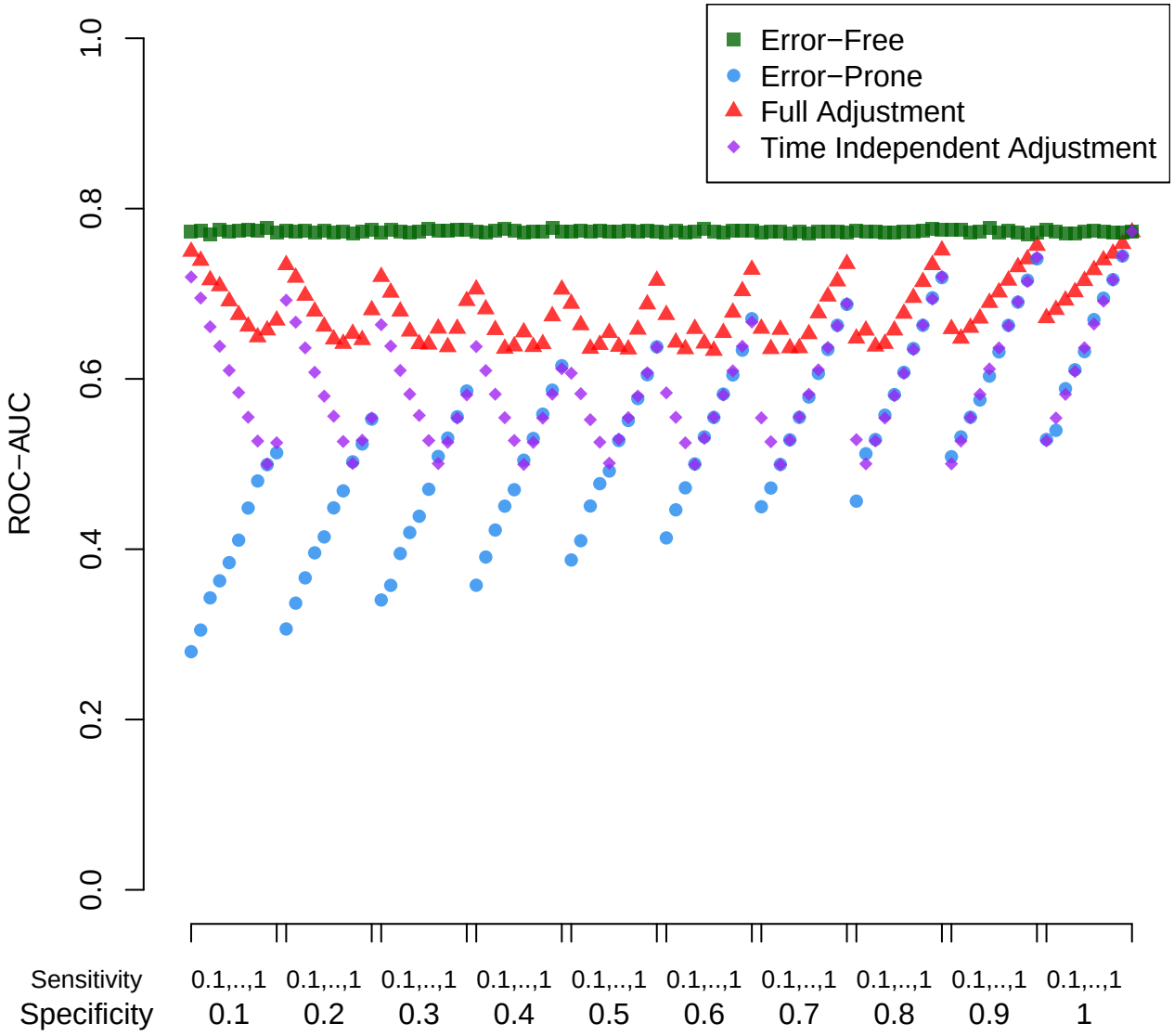

Figure 47: ROC-AUC for survival simulations under varying sensitivity and specificity rates, band width=0.7, n=1000.

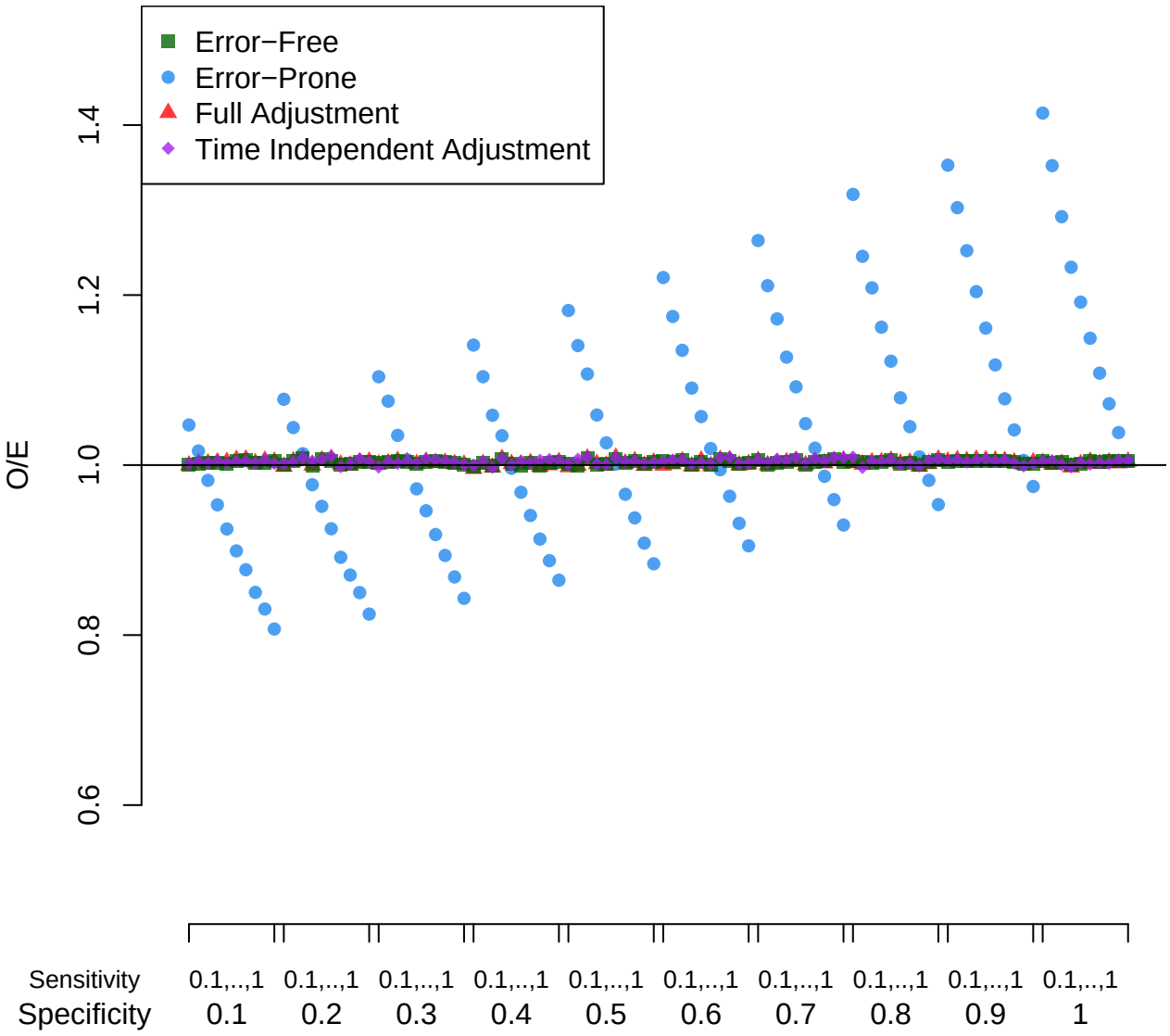

Figure 48: O/E ratios for survival simulations under varying sensitivity and specificity rates, band width=0.8, n=1000.

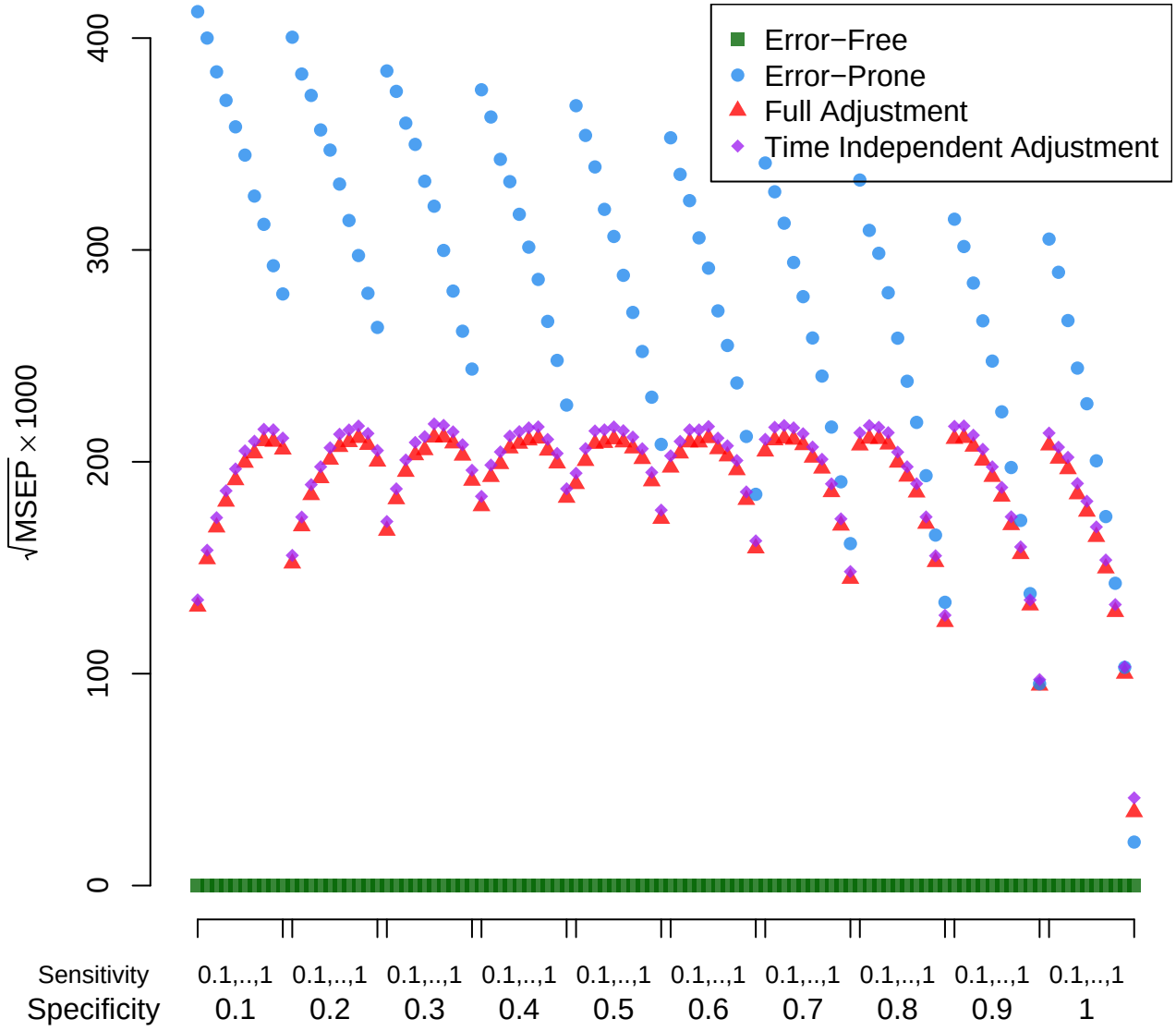

Figure 49: $\sqrt{MSEP} * 1000$ for survival simulations under varying sensitivity and specificity rates, band width=0.8, n=1000.

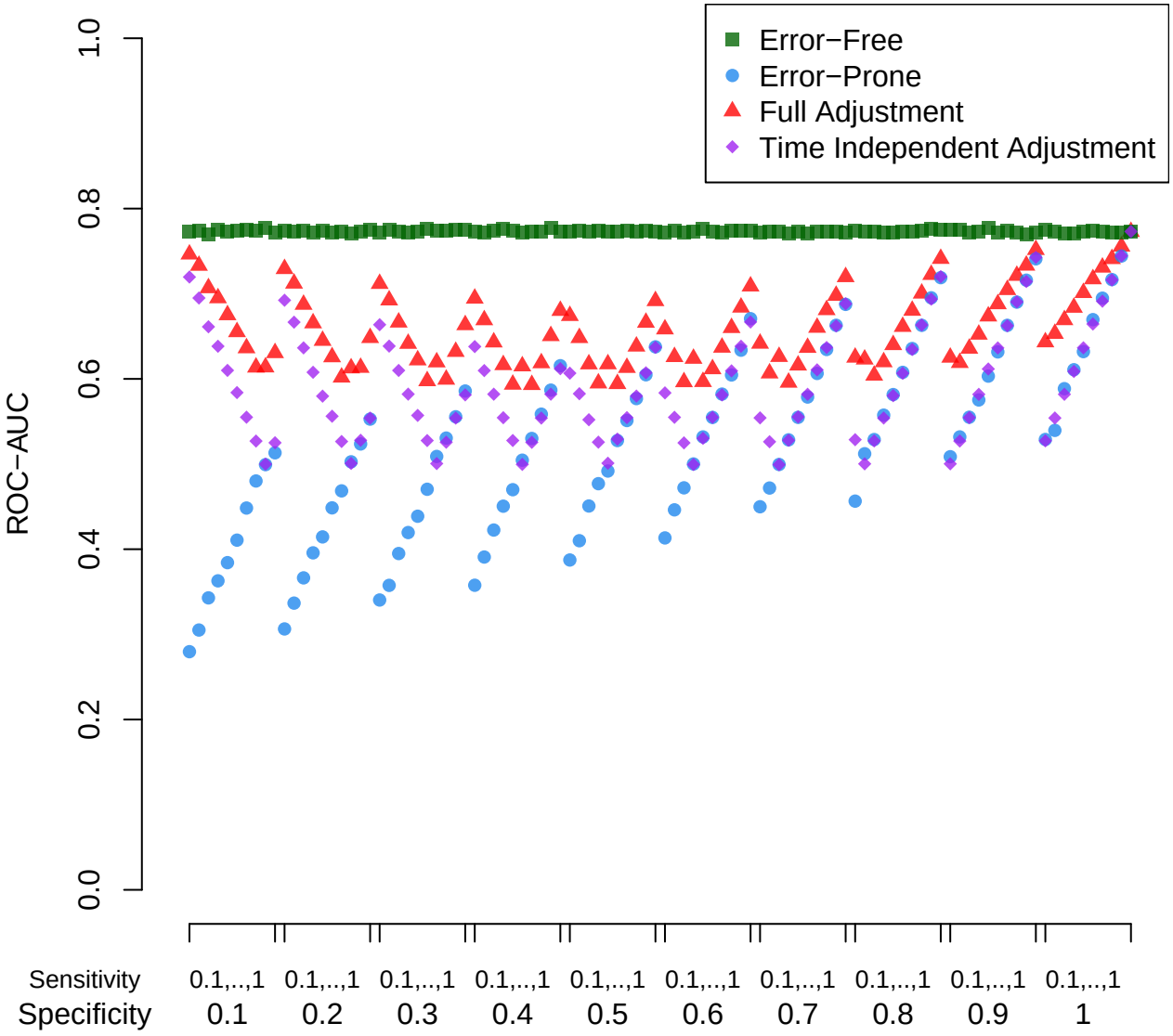

Figure 50: ROC-AUC for survival simulations under varying sensitivity and specificity rates, band width=0.8, n=1000.

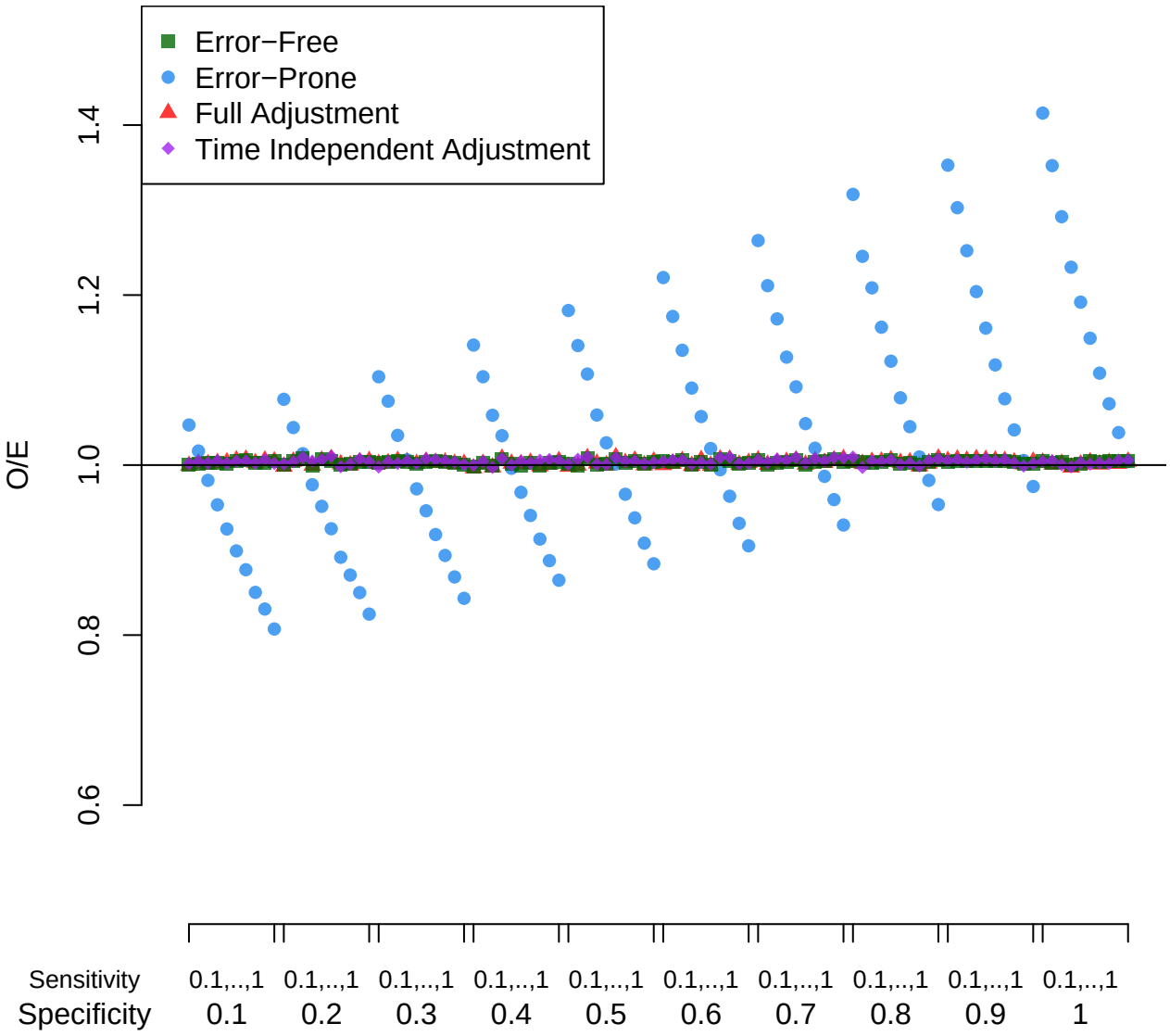

Figure 51: O/E ratios for survival simulations under varying sensitivity and specificity rates, band width=0.9, n=1000.

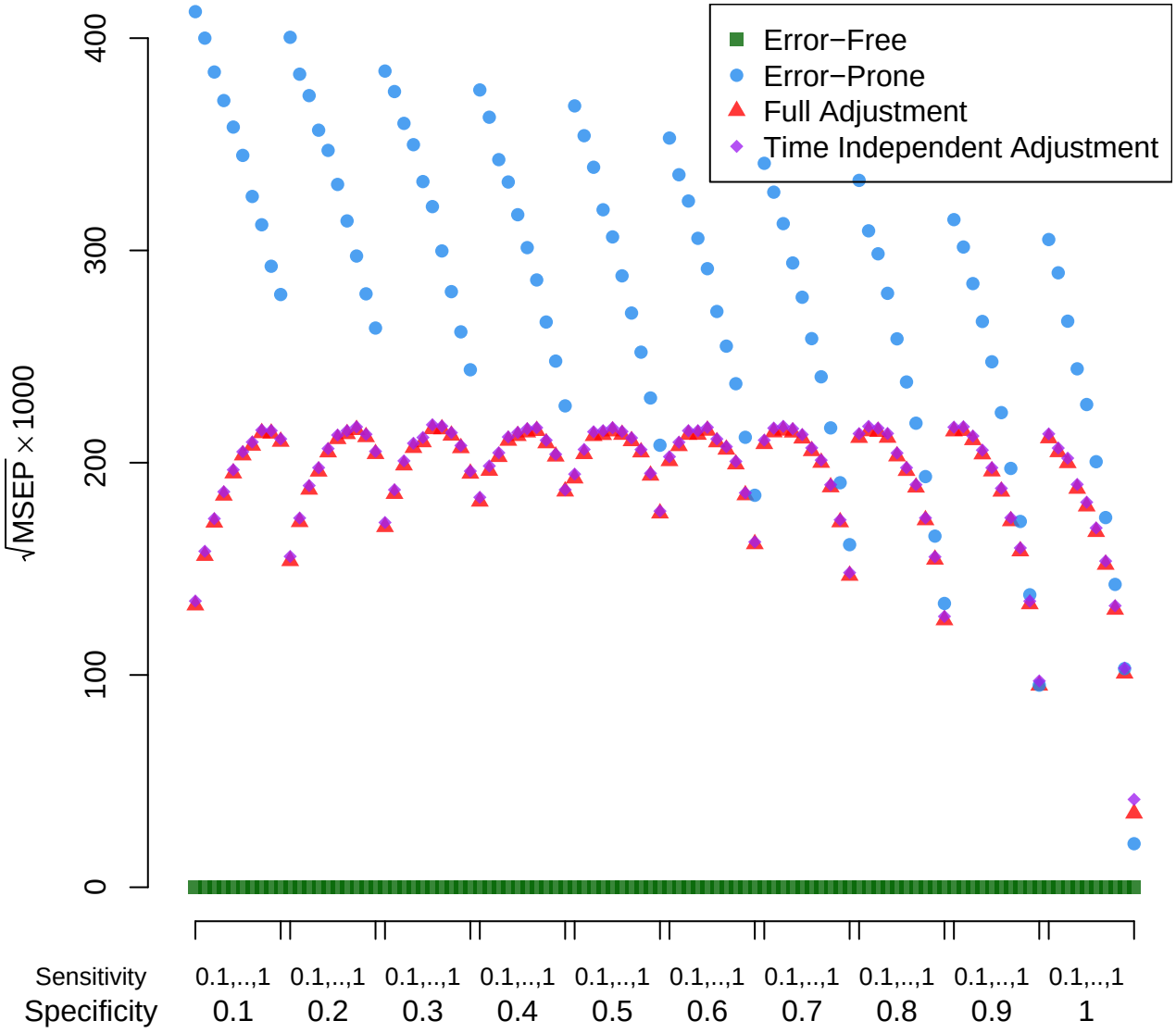

Figure 52: $\sqrt{MSEP} * 1000$ for survival simulations under varying sensitivity and specificity rates, band width=0.9, n=1000.

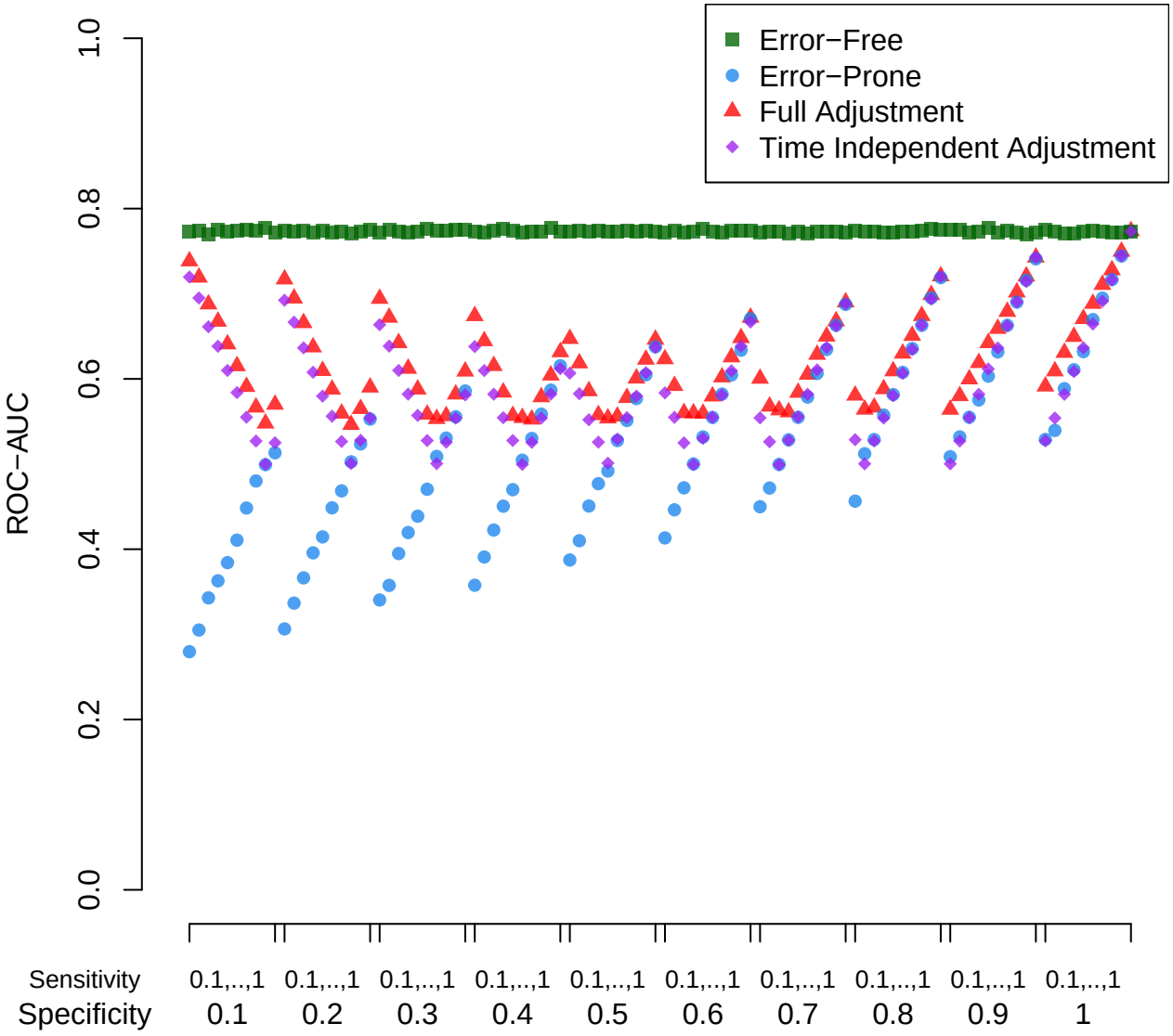

Figure 53: ROC-AUC for survival simulations under varying sensitivity and specificity rates, band width=0.9, n=1000.